Energy Dispersive X-ray Spectrometry: Physical Principles and User-Selected Parameters

J. Goldstein et al., *Scanning Electron Microscopy and X-Ray Microanalysis*,
https://doi.org/10.1007/978-1-4939-6676-9_16

16.1 The Energy Dispersive Spectrometry (EDS) Process

As illustrated in ▣ Fig. 16.1, the physical basis of energy dispersive X-ray spectrometry (EDS) with a semiconductor detector begins with photoelectric absorption of an X-ray photon in the active volume of the semiconductor (Si). The entire energy of the photon is transferred to a bound inner shell atomic electron, which is ejected with kinetic energy equal to the photon energy minus the shell ionization energy (binding energy), 1.838 keV for the Si K-shell and 0.098 keV for the Si L-shell. The ejected photoelectron undergoes inelastic scattering within the Si crystal. One of the consequences of the energy loss is the promotion of bound outer shell valence electrons to the conduction band of the semiconductor, leaving behind positively charged "holes" in the valence band. In the conduction band, the free electrons can move in response to a potential applied between the entrance surface electrode and the back surface electrode across the thickness of the Si crystal, while the positive holes in the conduction band drift in the opposite direction, resulting in the collection of electrons at the anode on the back surface of the EDS detector. This charge generation process requires approximately 3.6 eV per electron hole pair, so that the number of charge carriers is proportional to the original photon energy, E_p:

$$n = E_\mathrm{p} / 3.6\,\mathrm{eV} \tag{16.1}$$

For a Mn K-L_3 photon with an energy of 5.895 keV, approximately 1638 electron–hole pairs are created, comprising a charge of 2.6×10^{-16} coulombs. Because the detector can respond to any photon energy from a threshold of approximately 50 eV to 30 keV or more, the process has been named "energy dispersive," although in the spectrometry sense there is no actual dispersion such as occurs in a diffraction element spectrometer.

The original type of EDS was the lithium-drifted silicon [Si(Li)-EDS] detector (▣ Fig. 16.1a), with a uniform electrode on the front and rear surfaces (Fitzgerald et al. 1968). Over the last 10 years, the Si(Li)-EDS has been replaced by the silicon drift detector design (SDD-EDS), illustrated in ▣ Fig. 16.1b (Gatti and Rehak 1984; Struder et al. 1998). The SDD-EDS uses the same detection physics with a uniform front surface electrode, but the rear surface electrode is a complex pattern of nested ring electrodes with a small central anode. A pattern of potentials applied to the individual ring electrode creates an internal "collection channel," which acts to bring free electrons deposited anywhere in the detector volume to the central anode for collection. (Note that in some designs the small anode is placed asymmetrically on one side in a "teardrop" shape.)

The determination of the photon energy through the collection and measurement of this charge deposited in the detector requires an extremely sensitive and sophisticated electronic system, which operates automatically under computer control with only a limited number of parameters under the user's control, as described below under "Best Practices." The charge measurement in the detector provides the fundamental unit of information to construct the EDS spectrum, which is created in the form of a histogram in which the horizontal axis is a series of energy bins, and the vertical axis is the number of photons whose energy fits within that bin value. As shown in ▣ Fig. 16.2, from the user's point of view this process of EDS detection can be considered simply as a "black box" which receives the X-ray photon, measures the photon energy, and increments the spectrum histogram being constructed in the computer memory by one unit at the appropriate energy bin. The typical photon energy range that can be measured by EDS starts at a threshold of 0.05 keV and extends to 30 keV or even higher, depending on the detector design.

16.1.1 The Principal EDS Artifact: Peak Broadening (EDS Resolution Function)

If the EDS detection and measurement process were perfect, all the measurements for a particular characteristic X-ray peak would be placed in a single energy bin with a very narrow width. For example, the natural energy width of Mn K-L_3 is approximately 1.5 eV. However, the number of electron–hole pairs generated from a characteristic X-ray photon that is sharply defined in energy is nevertheless subject to natural statistical fluctuations. The number of charge carriers that are created follows the Gaussian (normal) distribution, so that the variation in the number of charge carriers, n, in repeated measurements of photons of the same energy is expected to follow $1\sigma = n^{1/2}$. The 1σ value for the 1638 charge carriers for the MnK-L_3 photon is approximately 40 electron-hole pairs, which corresponds to a broadening contribution to the peak width of 0.024 (2.4 %) which can be compared to the natural width of 1.5 eV/5895 eV (from ▣ Fig. 4.2), measured as the full peak width a half-maximum height (FWHM), or 0.00025 (0.025 %), which is a broadening factor of approximately 100. The EDS peak width (FWHM) measured experimentally is a function of the photon energy, which can be estimated approximately as (Fiori and Newbury 1978)

$$\mathrm{FWHM}(E) = \left[\left(2.5\left(E - E_\mathrm{ref}\right) + \mathrm{FHWM}_\mathrm{ref}{}^{2}\right)\right]^{1/2} \tag{16.2}$$

where FWHM(E), $\mathrm{FHWM}_\mathrm{ref}$, E and E_ref are expressed in electronvolts. The reference values for Eq. (16.2) can be conveniently taken from the values for Mn K-$L_{2,3}$ for a particular EDS system.

The EDS resolution function creates the principal artifact encountered in the measured EDS spectrum, which is the substantial broadening by a factor of 20 or more of the measured characteristic X-ray peaks, as shown in ▣ Fig. 16.3, where the peak markers (thin vertical lines) are approximately the true width of the Mn K-family characteristic X-ray peaks. Of course, all photons that are measured are

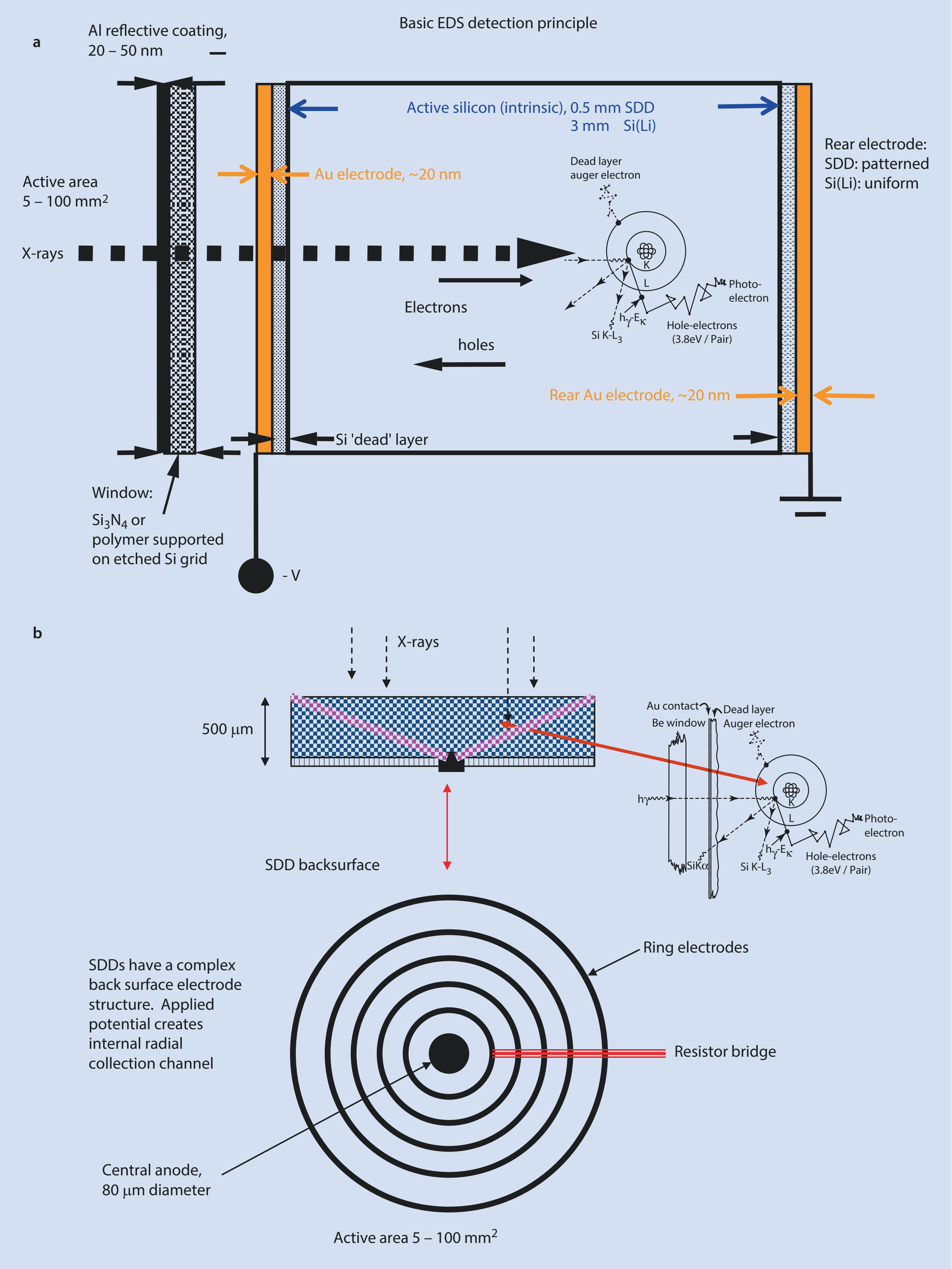

Fig. 16.1 **a** Basic principle of photon measurement with a semiconductor-based energy dispersive X-ray spectrometer. **b** Schematic of silicon drift detector (SDD) design, showing the complex patterned back surface electrode with a small central anode

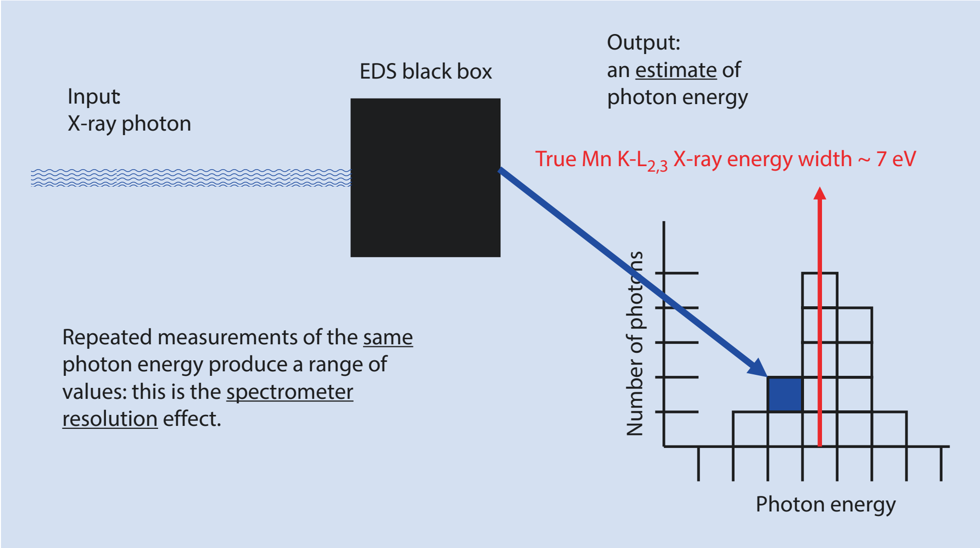

Repeated measurements of the same photon energy produce a range of values: this is the spectrometer resolution effect.

Fig. 16.2 "Black box" representation of the EDS detection and histogram binning process

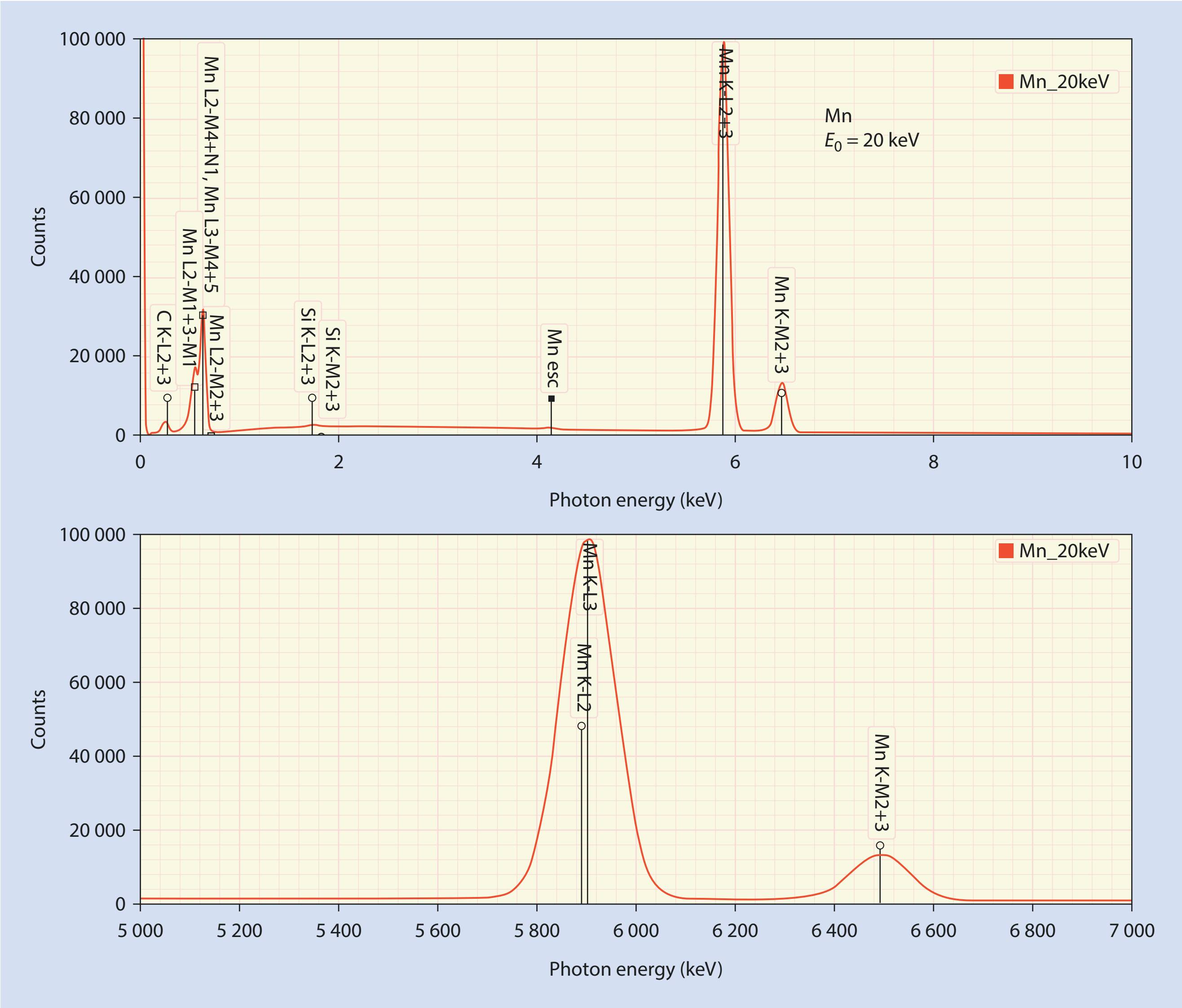

Fig. 16.3 SDD-EDS spectrum of Mn with $E_0 = 20$ keV and a time constant that produces a resolution of FWHM = 129 eV at Mn K-L$_{2,3}$

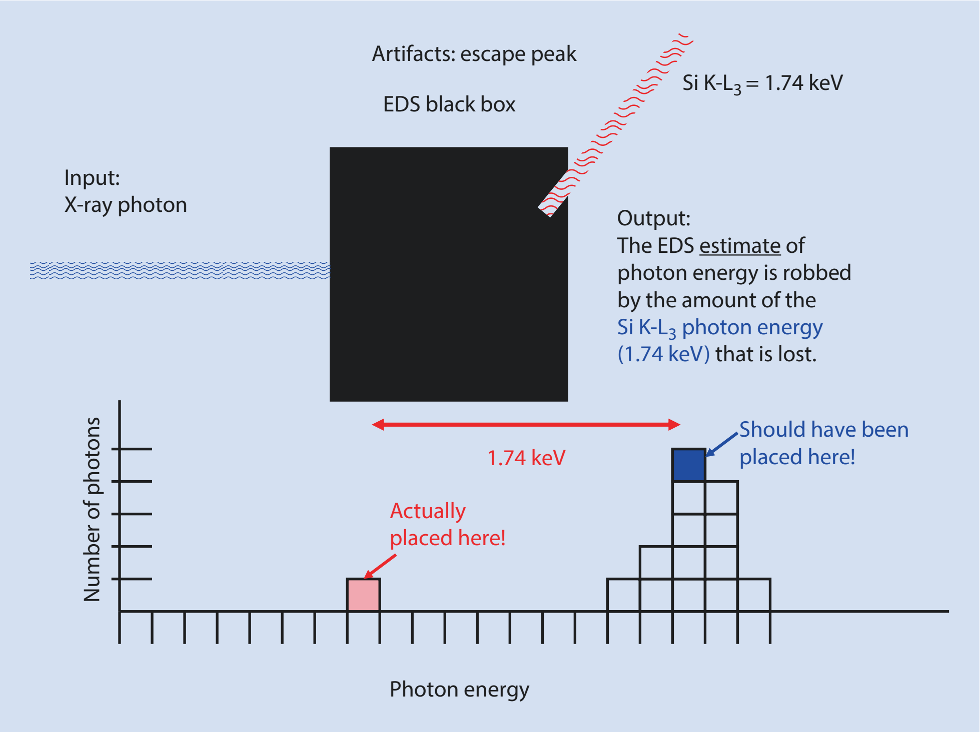

Fig. 16.4 EDS "black box" representation of the Si-escape peak artifact

subject to the EDS resolution function, including the X-ray *bremsstrahlung* (continuum) background, but because the continuum is created at all energies up to E_0 and because of its slow variation with photon energy, the distortions introduced into the continuum background by the EDS resolution function are more difficult to discern.

The major impact of peak broadening is the frequent occurrence in practical analytical situations of mutually interfering peaks that arise even with pure elements, for example, Si K-L$_3$ and Si K-M$_3$ and the Fe L-family. When mixtures of elements are analyzed, Interferences are especially frequent when elements with atomic numbers above 20 are present since these elements have increasingly complex spectra of L- and M- shell X-rays that have a wide energy span. A secondary impact of peak broadening occurs when trace elements are to be measured. Peak broadening has the effect of spreading the characteristic X-rays over a wide range of the X-ray continuum background. Variance in the background sets the ultimate limit of detection.

16.1.2 Minor Artifacts: The Si-Escape Peak

After photoelectric absorption by a silicon atom in the detector, the atom is left in an ionized excited state with a vacancy in the K- or L- shell. This excited state will decay by inter-shell electron transitions that result in the emission of a Si Auger electron (e.g., KLL), which will undergo inelastic scattering and contribute to the free charge generation, or in about 10 % of the events, a Si K-shell X-ray. This Si K-shell X-ray will propagate in the detector and in most cases will be undergo photoelectric absorption with the L-shell, ejecting another photoelectron and further contributing to the charge generation. However, in a small number of events, as illustrated schematically in Fig. 16.4, the Si K-shell X-ray will escape from the detector, carrying with it 1.740 keV (for a Si K-L$_3$ X-ray) and robbing the original photon being captured of this amount of energy, which creates an artifact peak at an energy corresponding to:

$$\text{Escape peak energy} = \text{Parent peak energy} - 1.740\,\text{keV} \quad \textbf{(16.3)}$$

Si-escape peaks are illustrated for tin and gold in Fig. 16.5. The intensity ratio of the Si-escape peak/parent peak depends on the energy of the parent photon, with a maximum value for this ratio occurring for photon energies just above the Si K-shell ionization energy (1.838 keV) and decreasing as the photon energy increases. It is important to identify Si-escape peaks so that they are not mistaken for elements present at minor or trace levels.

16.1.3 Minor Artifacts: Coincidence Peaks

Although the EDS spectrum appears to an observer to accumulate simultaneously at all energies, the EDS system is in fact only capable of processing one photon at a time, with a duty cycle that ranges from 200 ns to several microseconds, depending on the particular EDS. If a second photon should enter the detector during this measurement period, the photon energies would be added together, producing an artifact known as a "coincidence peak" or a "sum peak," as illustrated schematically in Fig. 16.6. An "anti-coincidence function" or "fast discriminator" is incorporated in the signal processing

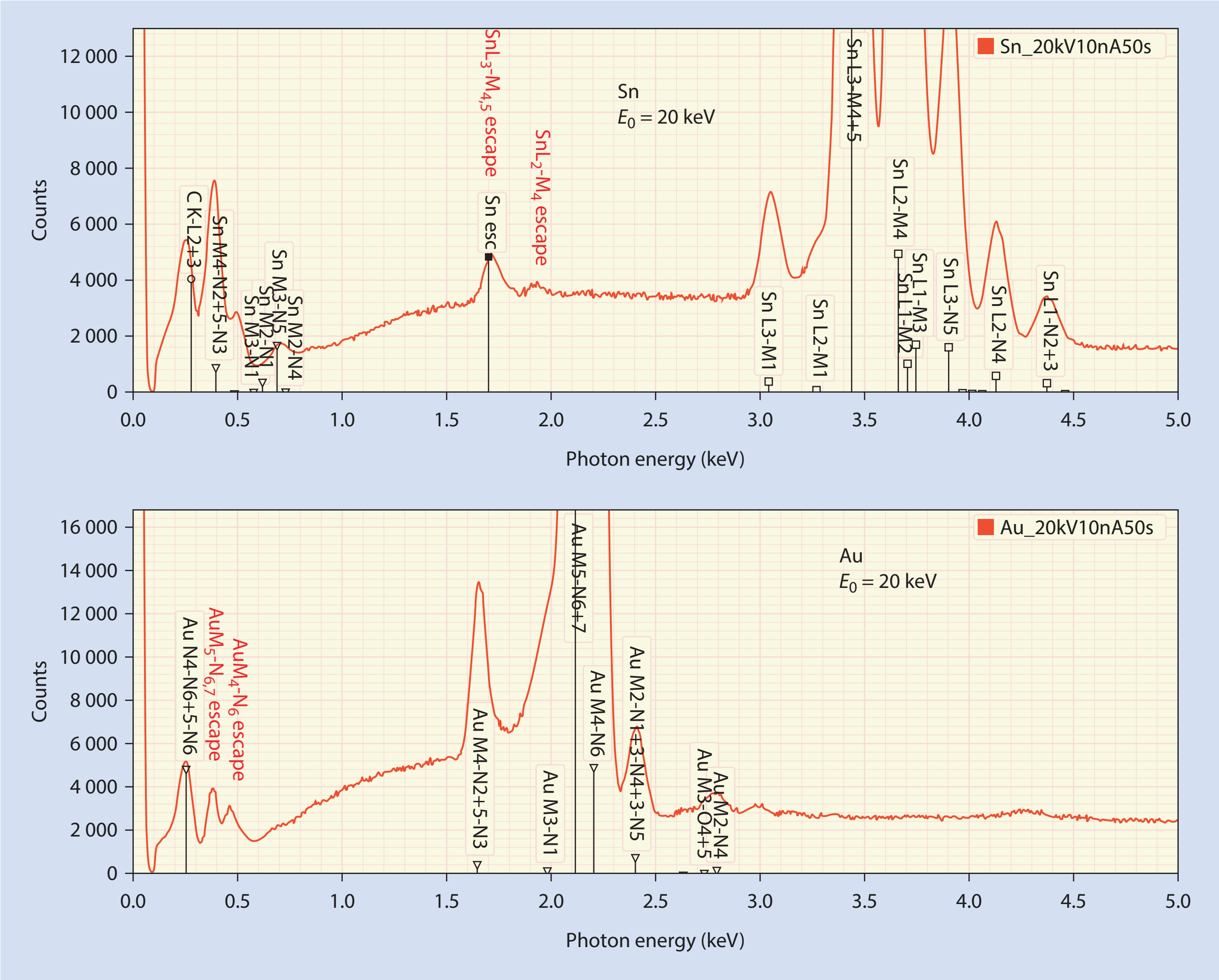

Fig. 16.5 Si-escape peaks observed with an SDD-EDS for Sn and Au (E_0 = 20 keV)

Fig. 16.6 EDS "black box" representation of photon coincidence

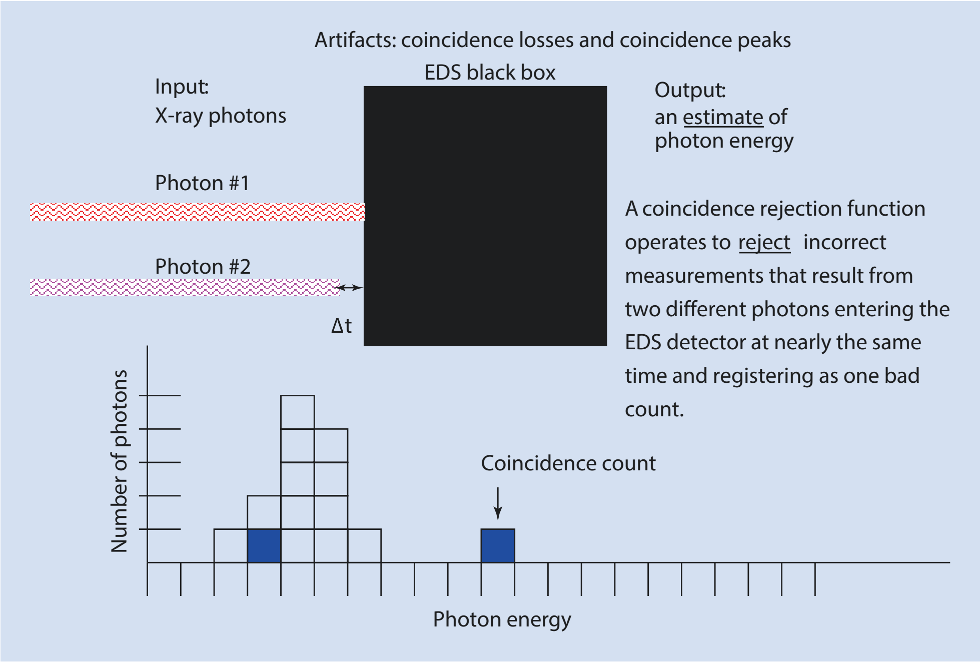

A coincidence rejection function operates to reject incorrect measurements that result from two different photons entering the EDS detector at nearly the same time and registering as one bad count.

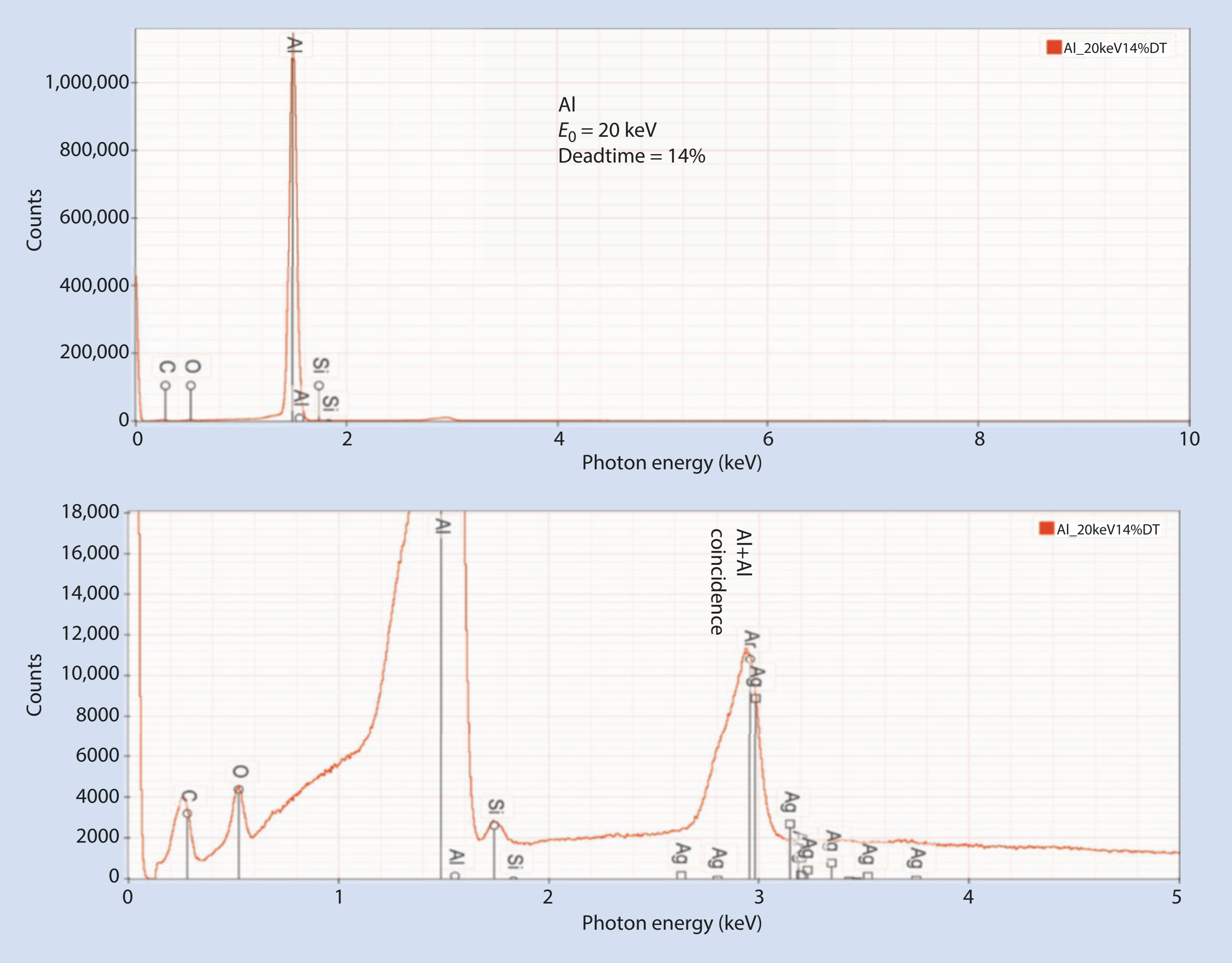

Fig. 16.7 Al at $E_0 = 20$ keV. Coincidence peak (Al + Al) observed at dead-time = 14 %. Note proximity of this artifact peak to Ar K-$L_{2,3}$ and Ag L-M family

chain to suppress this effect by rejecting the measurement of both photons, but as the flux of X-rays increases, an increasing frequency of events will occur in which the time separation between the two events is too short for the anti-coincidence function to recognize and reject the separate photons, resulting in an artifact sum photon. This coincidence phenomenon can occur between any two photons, for example, two characteristic X-rays, a characteristic X-ray plus a continuum X-ray, or two continuum X-rays. Coincidence produces a readily recognizable artifact peak when coincidence occurs between two photon energies that are particularly abundant, which is the case for high intensity characteristic X-ray peaks. An example is shown in Fig. 16.7, where two Al K-L_3 photons (1.487 keV) combine to produce a coincidence peak at 2.972 keV. Coincidence events can be formed from any two characteristic peaks, for example, O K-L + Si K-L_2. It is important to identify coincidence peaks so that they are not mistaken for characteristic peaks of elements present at minor or trace levels. Coincidence events involving lower energy photons will occur above the Duane–Hunt high energy limit (which corresponds to the incident beam energy, E_0) and should not be mistaken for the true limit.

16.1.4 Minor Artifacts: Si Absorption Edge and Si Internal Fluorescence Peak

X-rays entering the EDS must pass through a window, typically a thin polymer, which is often supported on an etched silicon grid. Some X-rays will be absorbed in this grid silicon, especially those whose photon energy is just above the Si K-ionization energy (1.839 keV). In addition, there is a thin inactive Si layer ("dead-layer") just below the entrance electrode of the EDS that also acts to absorb X-rays. The X-ray mass absorption coefficient of silicon increases abruptly at the K-shell ionization energy, and this has the effect of increasing the absorption of the X-ray continuum, producing an abrupt step. However, the EDS resolution function acts to broaden all photon energies so that this sharp feature is also broadened, as seen in Fig. 16.8 (after peak fitting for Si) and made into a

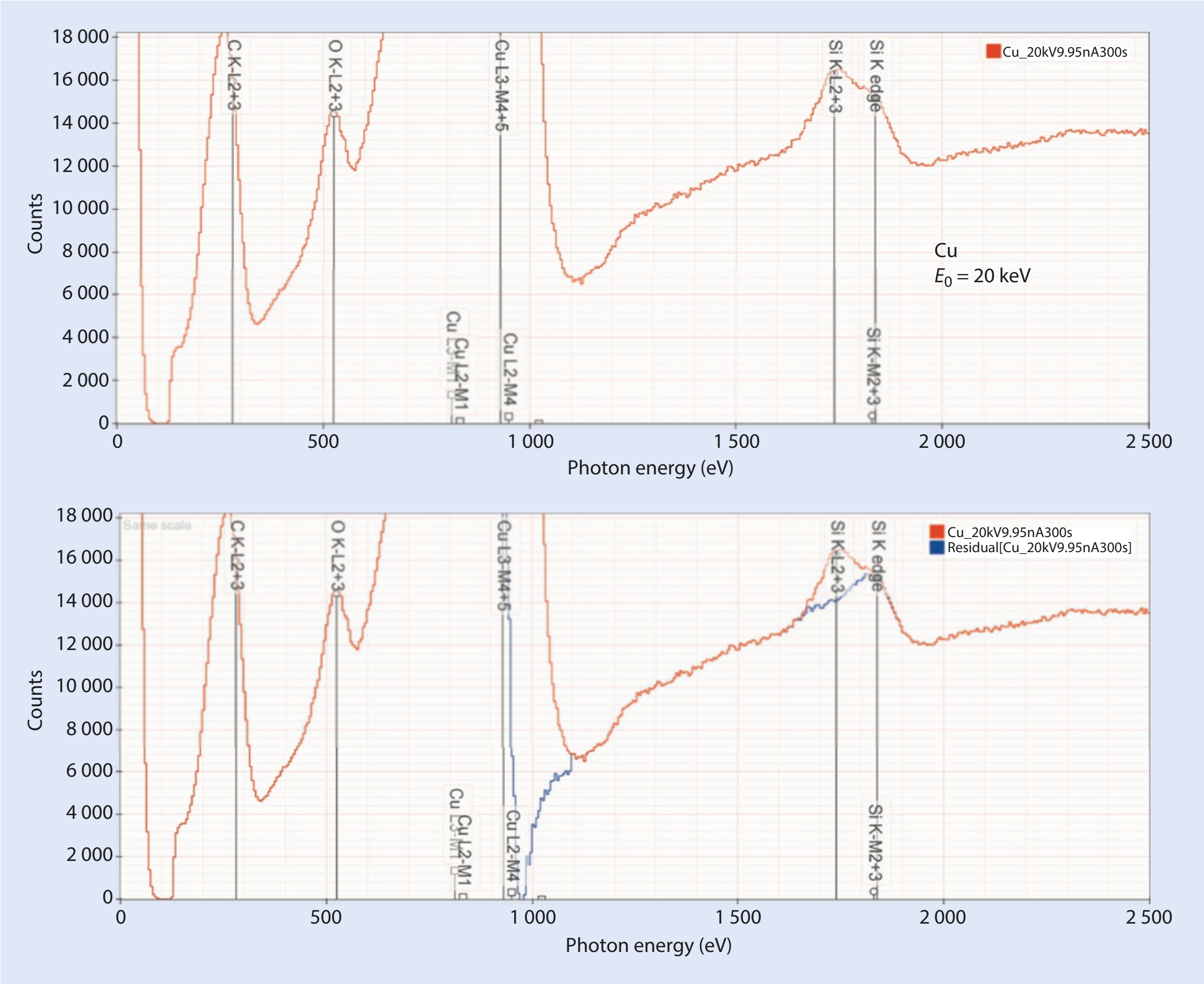

Fig. 16.8 Cu at $E_0 = 20$ keV. The artifact Si peak is a combination of the Si K-absorption edge and the Si internal fluorescence peak (peak fitting in lower spectrum) created by absorption of X-rays in the Si support grid and the Si detector dead-layer, and subsequent Si X-ray emission

peak-like structure. The absorption of X-rays by the Si grid and Si dead-layer ionizes Si atoms and subsequently results in the emission of Si K-shell X-rays, which contribute a false Si peak to the spectrum. In the example for a copper target shown in Fig. 16.8, the apparent level of Si contributed by the internal fluorescence artifact is approximately 0.002 mass fraction.

16.2 “Best Practices” for Electron-Excited EDS Operation

While modern EDS systems are well supported by computer automation, there remain parameters whose selection is the responsibility of the user.

16.2.1 Operation of the EDS System

Before commencing any EDS microanalysis campaign, the analyst should follow an established checklist with careful attention to the measurement science of EDS operation. To establish the basis for quantitative analysis, the EDS parameters must be chosen consistently, especially if the analyst wishes to use archived spectra to serve as standards.

Choosing the EDS Time Constant (Resolution and Throughput)

The EDS amplifier time constant (a generic term which may be locally known as “shaping time,” “processing time,” “resolution,” “count rate range,” “1–6,” etc.) should be checked. There are usually at least two settings, one that optimizes resolution (at the cost of X-ray throughput) and one that optimizes throughput (at the cost of resolution). Confirming the desired choice of the time constant is critical for consistent recording of spectra, especially if the analyst is using archived spectra to serve as standards for quantitative analysis. This is especially important when the EDS system is in a multi-user environment, since the previous user may have altered this parameter.

Channel Width and Number

The energy width of the histogram bins is typically chosen as 5, 10, or 20 eV. The bin energy width determines how many bins will define an X-ray peak. Since the peak width is a function of photon energy, as described by Eq. (16.2), decreasing from approximately 129 eV at Mn K-L3 (5.895 keV) to approximately 50 eV FWHM for C K-L$_2$ (0.282 keV), a selection of a 5-eV bin width is a useful choice to optimize peak fitting since this choice will provide 10 channels across C K-L$_2$. The number of bins that comprise the spectrum multiplied by the bin width gives the energy span. It is useful to capture the complete energy spectrum from a threshold of 0.1 keV to the incident beam energy, E_0. Thus, to span 0–20 keV with 5 eV bins requires 4096 channels.

Choosing the Solid Angle of the EDS

The solid angle Ω of a detector with an active area A at a distance r from the specimen is

$$\Omega = A / r^2 \tag{16.4}$$

If the EDS is mounted on a translatable slide that can alter the detector-to-specimen distance, then the user must select a specific value for this distance for consistency with archived standard spectra if these are to be used in quantitative analysis procedures. Because of the exponent on the distance parameter r in Eq. (16.4), a small error in r propagates to a much larger error in the solid angle and a proportional deviation in the measured intensity.

Selecting a Beam Current for an Acceptable Level of System Dead-Time

X-rays are generated randomly in time with an average rate determined by the flux of electrons striking the specimen, thus scaling with the incident beam current. As discussed above, the EDS system can measure only one X-ray photon at a time, so that it is effectively unavailable if another photon arrives while the system is "busy" measuring the first photon. Depending on the separation in the time of arrival of the second photon, the anti-coincidence function will exclude the second photon, but if the measurement of the first photon is not sufficiently advanced, both photons will be excluded from the measurement and effectively lost. Due to this photon loss, the output count rate (OCR) in counts/second of the detector will always be less than the input count rate (ICR). The relation between the OCR and ICR is shown in Fig. 16.9 for a four-detector SDD-EDS. An automatic correction function measures the time increments when the detector is busy processing photons, and to compensate for possible photon loss during this "dead-time," additional time is added at the conclusion of the user-specified measurement time so that all

Fig. 16.9 Output count rate versus input count rate for a four-detector SDD-EDS

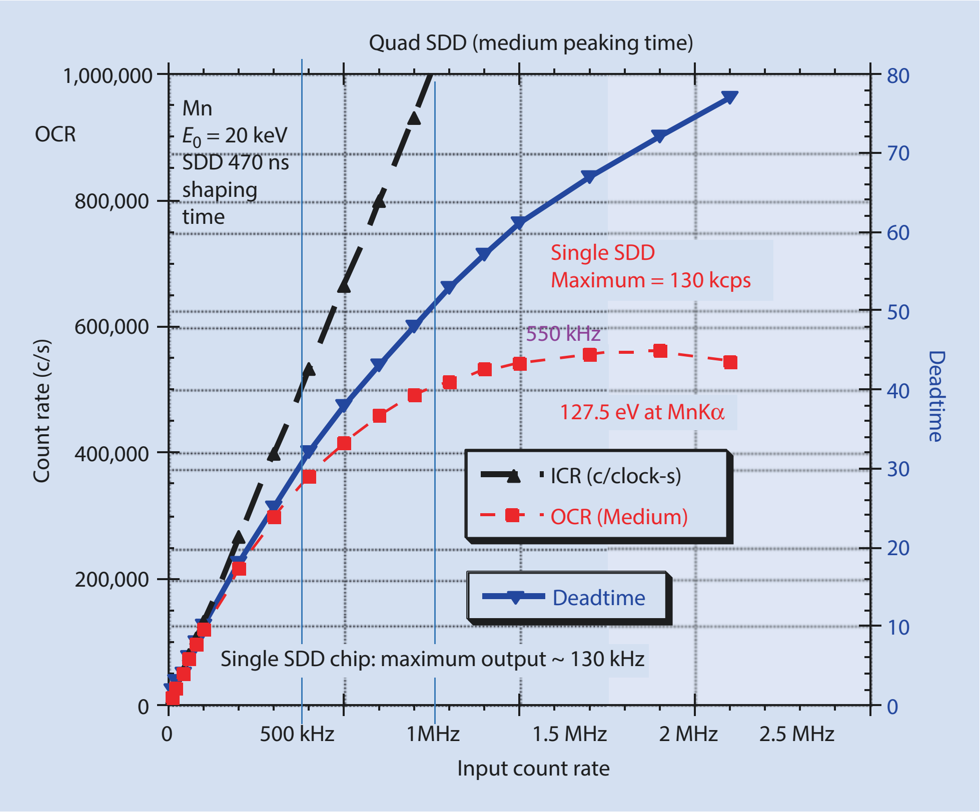

measurements are made on the basis of the same "live-time" so as to achieve constant dose for quantitative measurements. The level of activity of the EDS is reported to the user as a percentage "dead-time":

$$\mathrm{Deadtime}(\%)=\left[(\mathrm{ICR}-\mathrm{OCR})/\mathrm{ICR}\right]\times 100\% \qquad (16.5)$$

Dead-time increases as the beam current increases. The dead time correction circuit can correct the measurement time over the full dead-time range to 80 % or higher. (Note that as a component of a quality measurement system, the dead-time correction function should be periodically checked by systematically changing the beam current and comparing the measured X-ray intensity with predicted.) However, as the dead-time increases and the arrival rate of X-rays at the EDS increases, coincidence events become progressively more prominent. This effect is illustrated in ◘ Fig. 16.10 for a sequence of spectra from a glass with six peaks for O, Mg, Al, Si, Ca, and Fe.

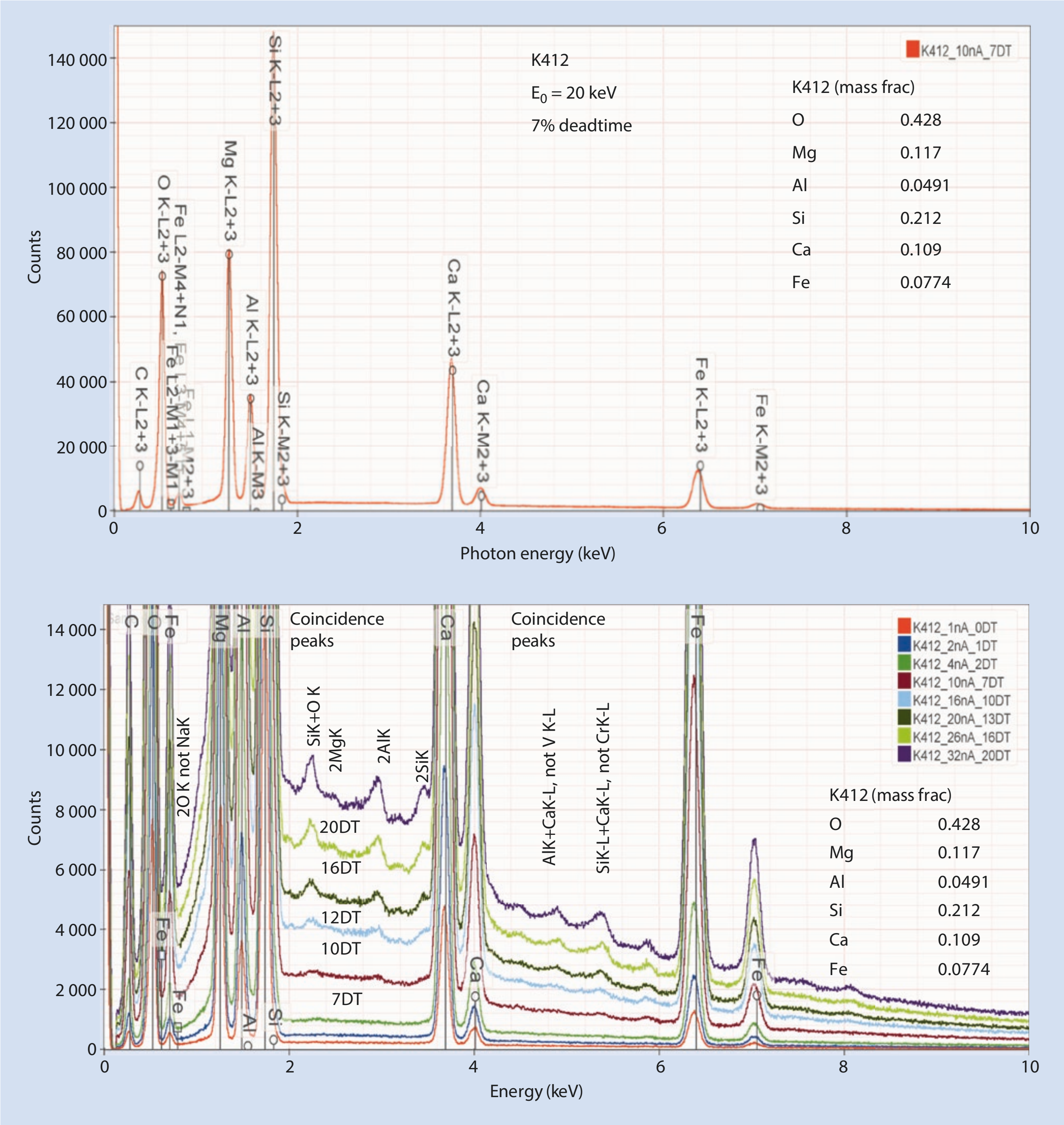

◘ **Fig. 16.10** Development of coincidence peaks as a function of dead-time. NIST Standard Reference Material SRM 470 (Mineral Glasses) K412. (*upper*) SDD-EDS spectrum at 7 % dead-time showing the characteristic peaks for O, Mg, Al, Si, Ca, and Fe. (*lower*) SDD-EDS spectra recorded over arrange of dead-times showing in-growth of coincidence peaks. Note elemental misidentifications that are possible major constituents (O, Mg, Al, Si, Ca, and Fe) measured at increasing dead-time. The spectra show the in-growth of a series of coincidence peaks as the dead-time increases. With the long pulses of the Si(Li) EDS technology, the pulse inspection function was effective in minimizing coincidence effects to dead-times in the range 20–30 %. There is more vendor-to-vendor variability in SDD-EDS technology. Some vendors provide coincidence detection that will permit dead-times of up to 50 %, while others are restricted to 10 % dead-time. Since there is variability among vendors' SDD performance, it is useful to perform a measurement to determine the performance characteristic of each detector. See the sidebar for a procedure implementing such a procedure. Regardless of dead-time restrictions, an SDD-EDS is still a factor of 10 or more faster than an Si(Li)-EDS for the same resolution. In summary, as a critical step in establishing a quality measurement strategy, the beam current (for a specific EDS solid angle) should be selected to produce an acceptable rate of coincidence events in the worst-case scenario. This beam current can then be used for all measurements with reasonable expectation that the dead-time will be within acceptable limits.

▪▪ Sidebar: Protocol for Determining the Optimal Probe Current and Dead-Time

Aluminum produces one of the highest fluxes of X-rays per unit probe current: With the Al K-shell ionization energy of 1.559 keV, a modest beam energy of 15 keV provides an overvoltage of 9.6 for strong excitation. Al K-L_2 is of sufficient energy (1.487 keV) that it has low self-absorption, and at this energy the SDD efficiency is also relatively high. The Al K-L_2 energy is low enough that this peak is also quite susceptible to coincidence events. Pure aluminum thus makes an ideal sample for testing the coincidence detection performance of a detector and for determining the maximum practical probe current for a given beam energy.

1. Place a mounted, flat, polished sample of pure Al in the SEM chamber at optimal analytical working distance.
2. Mount a Faraday cup with a picoammeter in the SEM chamber.
3. Configure the detector at the desired process time.
4. Configure the SEM at the desired beam energy and an initial probe current. Measure the probe current using the Faraday cup/picoammeter.
5. Collect a spectrum from the pure Al sample with at least 10,000 counts in the Al K peak.
6. Use your vendor's software (or NIST DTSA-II) to integrate the background-corrected intensity in the Al K peak ($E = 1.486$ keV).
7. Use your vendor's software (or NIST DTSA-II) to look for and integrate the background-corrected intensity in the Al K + Al K coincidence peak ($E = 2.972$ keV).
8. Determine the ratio of the integrated intensity I(Al K + Al K)/I(Al K). We desire this ratio to be smaller than 0.01 (1 %). In some trace analysis situations, it may desirable to have this ratio less than 0.001 (0.1 %). Setting this limit too low will limit throughput but setting it too high may make trace element analysis challenging.
9. If the ratio is too large, decrease the probe current and re-measure the probe current and the Al spectrum. Re-measure the ratio I(Al K + Al K)/I(Al K).
10. Repeat steps 5–10 until a suitable probe current has been determine.
11. Finally, note the suitable probe current and use it consistently at the beam energy for which it was determined.

16.3 Practical Aspects of Ensuring EDS Performance for a Quality Measurement Environment

The modern energy dispersive X-ray spectrometer is an amazing device capable of measuring the energy of tens of thousands of X-ray events per second. The spectra can be processed to extract measures of composition with a precision of a fraction of a weight-percent. However, this potential will not be realized if the detector is not performing optimally. It is important to ensure that the detector is mounted and configured optimally each time it is used. Some parameters change infrequently and need only be checked when a significant modification is made to the detector or the SEM. Other parameters and performance metrics can change from day-to-day and need to be verified more frequently. The following sections will step through a series of tests in a rationally ordered progression. The initial tests and configuration steps need only be performed occasionally, for example, when the detector is first commissioned or when a significant service event has occurred. Later steps, like ensuring proper calibration, should be performed regularly and a archival record of the results maintained.

16.3.1 Detector Geometry

In most electron-beam instruments, the EDS detector is mounted on a fixed flange to ensure a consistent sample/detector geometry with a fixed elevation angle. Almost all modern EDS detectors are mounted in a tubular snout with the crystal mounted at the end of the snout and the face of the active detector element perpendicular to the principle axis of the snout. The principal axis of the snout is oriented in the instrument such that it intersects with the electron beam axis at the "optimal working distance." This geometry is illustrated in ▫ Fig. 16.11.

Often the detector is mounted on the flange on a sliding mechanism that allows the position of the detector to translate (move in and out) along the axis of the snout. The elevation angle is nominally held fixed during the translation but the distance from the detector crystal changes and along with it the solid angle (Ω) subtended by the detector. The solid

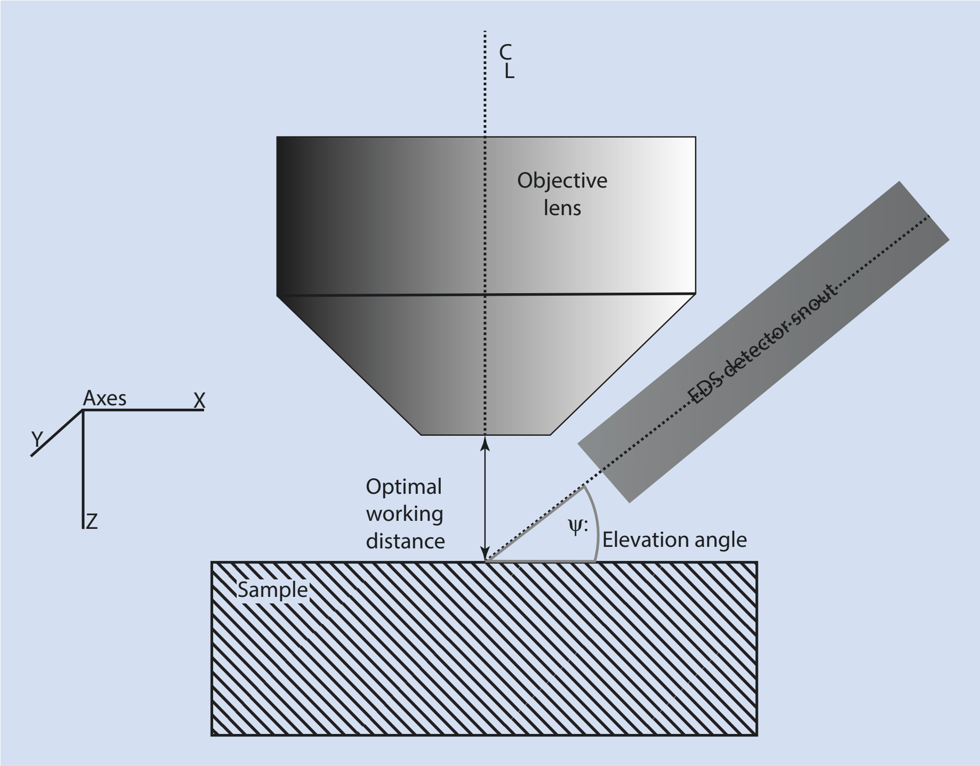

Fig. 16.11 The elevation angle is a fixed property of the instrument/detector

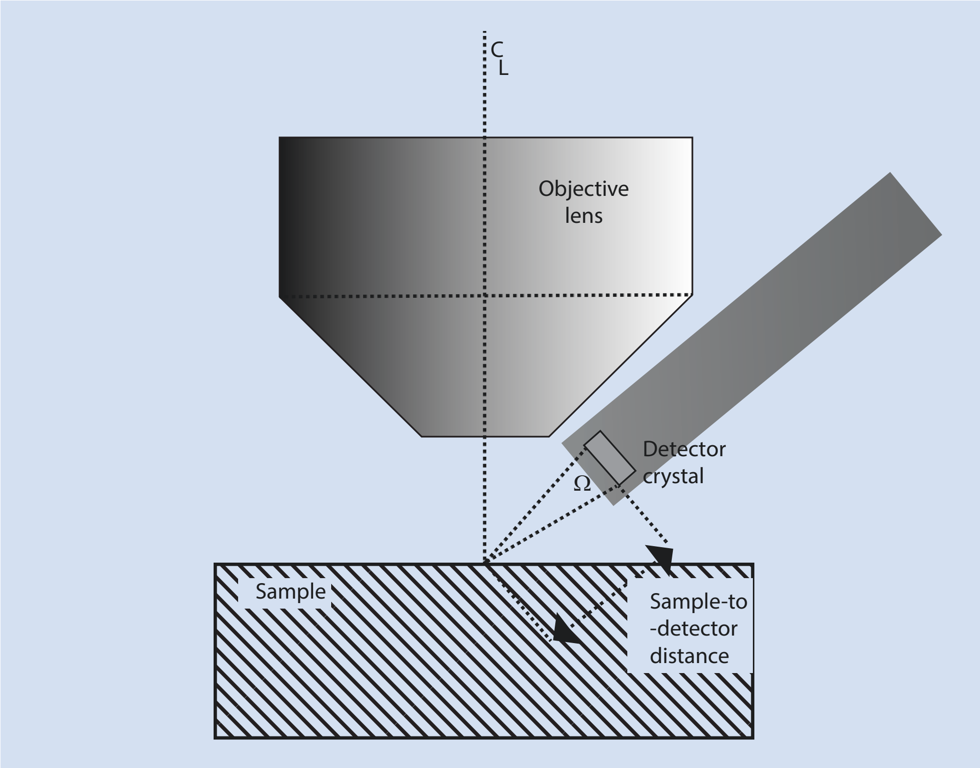

Fig. 16.12 The solid angle is a function of sample-to-detector distance and the active detector area

angle is illustrated in the Fig. 16.12. Moving the detector away from the sample is designed to decrease the solid angle but does not change the elevation angle or the optimal working distance.

It is important to be able to maintain a reproducible solid angle through consistent repositioning of the detector. Some slide mechanisms are motorized. Motorized mechanisms should define an “inserted” position and a “retracted” position, which you should test to ensure that the positioning is reproducible between insertions. Manual mechanisms usually provide a threaded screw with a manual crank to pull the detector in and out. The threaded screw will usually have a pair of interlocking nuts which can be positioned to define a consistent insertion position. The procedure in the sidebar below will allow you to set and maintain a constant solid angle and thus also a consistent detector collection efficiency.

Sidebar: Setting a Constant Detector-to-Sample Distance to Maintain Solid Angle

1. Locate the pair of lock nuts on the screw mechanism. Move the lock nuts to the inner most position on the treaded rod.
2. Insert the detector as close to the sample as possible. Ensure that the detector does not touch the interior of the microscope. The detector snout must be electrically isolated (no conductive path) from the interior of the chamber to eliminate noise caused by electrical ground loops.
3. Twist the upper lock nut to limit the motion of the detector towards the sample. Tighten the lower nut to lock the upper nut into position.
4. Test the reproducibility of the insertion point by extracting and inserting the detector and collecting a series of spectra. If the characteristic peak intensities are reproducible (to much better than a fraction of a percent) between insertions, the precision is adequate.

The take-off angle is the angle at which X-rays exit a flat sample in the direction of the detector. For a flat sample mounted perpendicular to the electron beam at the optimal working distance, the take-off angle equals the elevation angle. If the sample is tilted or the sample surface is at a slightly different working distance, then the take-off angle can be computed from the sample tilt, the working distance and the sample-to-detector distance. This is shown in ▣ Fig. 16.13. Often you will hear the terms elevation angle and take-off angle used interchangeably. It is more precise however to think of the elevation angle as being a fixed property of the instrument/detector geometry and the take-off angle being dependent upon instrument-specimen configuration.

Check 1: Verify the Elevation Angle

It is critical that your quantitative analysis software has the correct elevation/take-off angle. Matrix correction algorithms use the take-off angle to calculate the correct absorption

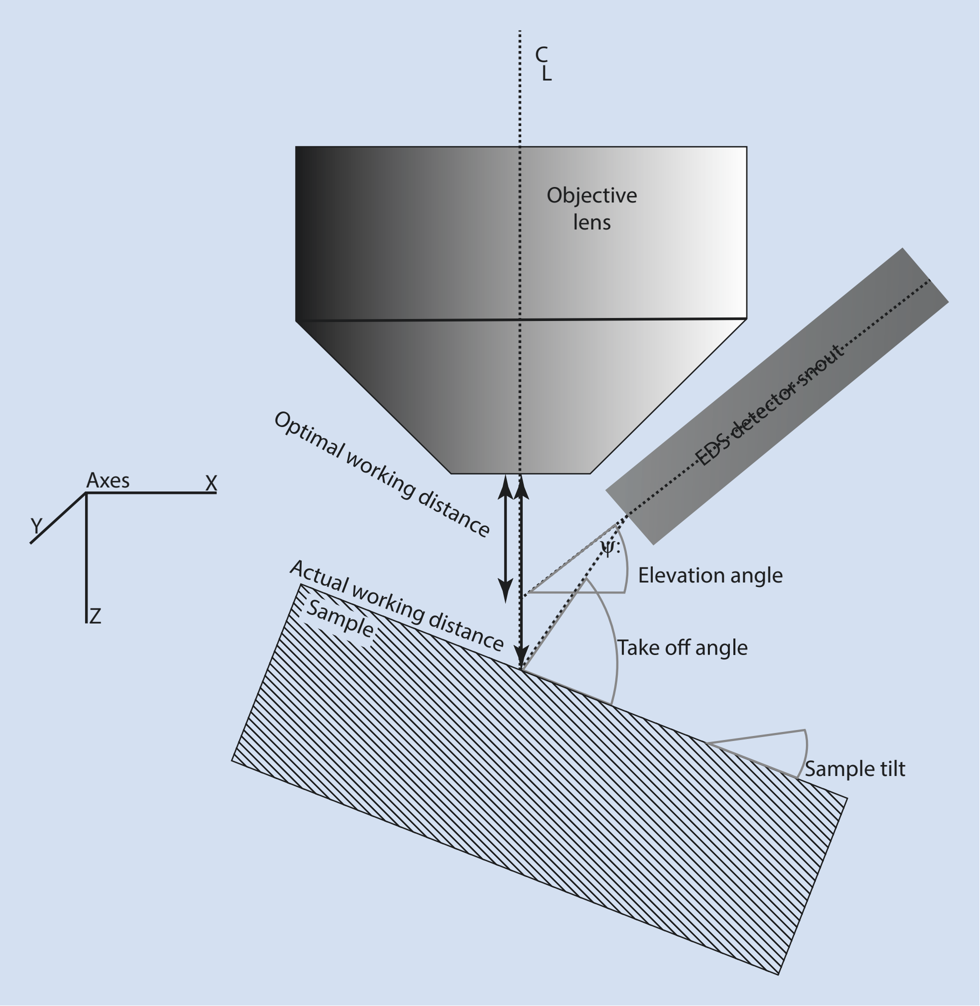

▣ **Fig. 16.13** The take-off angle is a function of the elevation angle, the sample tilt and the actual working distance

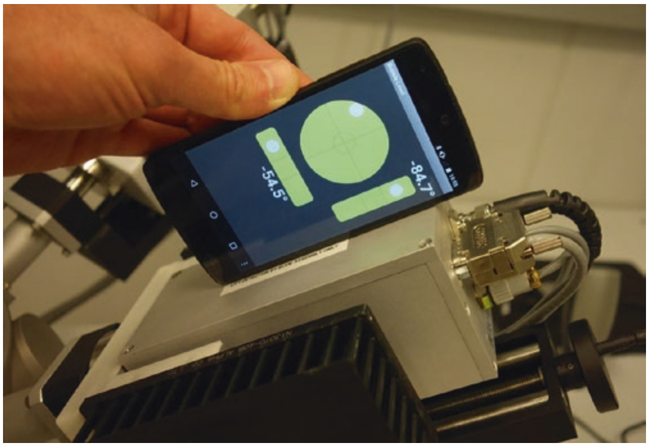

Fig. 16.14 Using a cell phone inclinometer to measure the elevation angle

correction. The elevation angle (usually sloppily called the "take-off angle") is often a configuration option that may be available to you to modify or may require a service engineer. Usually you can check the elevation angle by opening a spectrum data file in a text editor. Most spectrum files are ASCII text files and the vendors write a line containing the elevation or nominal take-off angle.

Compare the value produced by the software with the physical position of your detector relative to the beam axis. Sometimes, the correct instrument specific value of the take-off angle will be handwritten in the EDS vendor's documentation. Other times, you can extract the angle from instrument specific schematic diagrams from the SEM or EDS vendors. Regardless, it is a good idea to verify the elevation angle using a protractor or a smart phone. Many smart phones contain inclinometers which are accurate to within a degree and "bubble level apps" are available to turn the phone into a digital inclinometer. First, test the accuracy of the cell phone inclinometer using a 30-60-90 triangle or similar reference shape. Then use the cell phone to measure the angle of the snout relative to the angle of the column and calculate the elevation angle. Figure 16.14 shows that a cell phone measures the elevation angle of this detector to within half a degree (90°–54.5° = 35.5° ~ 35° nominal value). Achieving similar accuracy with a protractor and a bubble level is difficult.

16.3.2 Process Time

The "process time" (also called the "throughput setting," the "detector time constant," the "resolution setting" or other names) determines how much time the detector electronics dedicates to processing each incoming X-ray. A longer "process time" tends to produce lower X-ray throughput but higher spectral resolution. Shorter "process times" tend to produce higher X-ray throughput but lower spectral resolution. By throughput, we mean the maximum number of X-rays that the detector can measure per unit time. By spectral resolution we mean the width of a characteristic peak, usually taken to be the Mn K-$L_{2,3}$ (Kα) peak.

Higher throughput is desirable because it allows you to use higher probe currents to produce more X-rays and produce measured spectra with a larger number of measured X-rays. Higher resolution is desirable because it becomes easier to distinguish characteristic peaks of similar energy. Both are virtues but one is achieved at the expense of the other.

The task of selecting a process time is the task of balancing good throughput with adequate resolution. At the best resolution settings, throughput is seriously compromised and as a result the precision of quantitative analysis is also compromised. At the highest throughput settings, resolution is compromised and it becomes much more difficult to distinguish interfering peaks.

Fortunately, resolution degrades relatively slowly while throughput increases quickly. Moderate pulse process times tend to degrade the ultimate resolution by a few percent, while increasing throughput by much larger factors. Every vendor is different but typically a moderate pulse process time will produce both adequate resolution and excellent throughput.

While some modern SDD are capable of ultimate resolutions of 122–128 eV, compromising the resolution to 130–135 eV will produce an excellent compromise between resolution and throughput. Even a resolution of 140–150 eV at high throughputs can produce excellent quantitative results because the precision of spectrum fitting is more determined by the number of measured X-rays than the spectral resolution.

- **Check 2: Selecting a Process Time**
  - Ensure that your EDS detector electronics are set to a moderate process time that produces a good throughput with a resolution within 5 eV of the best resolution. Record this parameter in your electronic notebook for future reference.
  - Do not use an "adaptive process time" for standards-based quantitative analysis. Adaptive process times allow the resolution to change with throughput making spectrum fitting challenging and less accurate.

The optimization of throughput is also confounded by an another practical limitation—coincident X-rays or pulse-pileup—and will be addressed in a later section.

16.3.3 Optimal Working Distance

Nominally, the optimal working distance should be specified in instrument schematics. However, it is worth checking because it may vary slightly or there may be a mistake in design or manufacturing. From the detector geometry section, we know that the optimal working distance is the distance at which the axis along the detector snout intersects with the electron beam axis (see ◘ Fig. 16.13). This working distance should also produce the largest flux of X-rays and be the distance which is least sensitive to slight errors in vertical positioning.

- **Check 3: Measuring the Optimal Working Distance**

1. Select a sample like a piece of copper and mount it perpendicular to the electron beam axis.
2. Select a beam energy of 15–25 keV and a moderate probe current to produce ~ 20% dead time.
3. Move the stage's vertical axis to place the sample close to the objective lens pole piece. Be careful not to run the sample into a detector.
4. Focus the image and record the working distance reported by your SEM's software.
5. Collect a 60 live-time second spectrum.
6. Move the stage away from the objective lens pole piece in 1-mm steps.
7. Repeat steps 4–6, taking the working distance through the nominal optimal working distance.
8. Process the spectra. Extract the total number of counts in the energy range from about 100 eV to the beam energy and plot this number against the working distance.
9. Determine the working distance which produces the largest number of counts. Since this working distance represents an inflection point, the slope will be minimum and thus the sensitivity with respect to working distance will also be minimized.

16.3.4 Detector Orientation

In the previous section, we assumed that the principal axis of the detector snout is oriented to intersect with the electron beam axis. In other words, the detector points towards the sample. It is usually the EDS vendor's responsibility to ensure that the mounting flange has been designed to correctly orient and position the detector. The next check will verify this.

The active face of an EDS detector is a planar area that is mounted perpendicular to the snout axis. In front of the detector element there is usually a window and an electron trap. Most windows are ultrathin layers of polymer or silicon nitride mounted on a grid for mechanical strength. Examples of two support grids are given in ◘ Fig. 16.15. While the grid may have an open area fraction of 75–80 %, the silicon or carbon grid bars are often very thick (0.38 mm) to enhance mechanical rigidity under the strain of up to one atmosphere of differential pressure. Off-axis the grid bars can occlude the direct transmission of X-rays from the sample to the detector element. Furthermore, the magnetic electron trap can also occlude X-rays from off-axis. As a result, an EDS detector is more sensitive to X-rays produced on the snout axis than slightly off the axis. The result is a position dependent efficiency which peaks on axis and decreases as the source of the X-rays is further from axis.

A wide field-of-view X-ray spectrum image can demonstrate the position sensitivity and can be used to ensure that the detector snout and detector active element are oriented correctly.

- **Check 4: Collect a Wide Field X-ray Spectrum Image**

1. Mount a flat, polished piece of Cu in your SEM.
2. Image the Cu at the optimal working distance and at 20–25 keV to excite both the K and L lines.
3. Find out how wide a field-of-view your SEM can image at the optimal working distance. The example in ◘ Fig. 16.16 uses a 4-mm field-of-view.
4. Collect a high count X-ray spectrum image from the Cu. Acquiring at a moderate-to-high probe current for an hour or more at 256 × 256-pixel image dimensions should produce sufficiently high signal-to-noise data.
5. Process the data to extract and plot the raw intensities at each pixel in each of the Cu K-$L_{2,3}$ and Cu L-family lines.
    1. It is important to extract the raw intensities and not the normalized intensities since we are looking for variation in the raw intensity as a function of position.
    2. The open source software ImageJ-Fiji (ImageJ plus additional tools) can be used to process spectrum image data if it can be converted to a RAW format.

	AP3	AP5
Thickness (µm)	380	265
Rib width (µm)	59	45
Opening width (µm)	190	190
Open area %	76%	78%
Acceptance angle	53°	72°

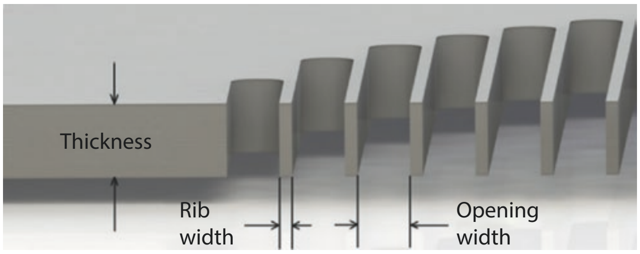

◘ **Fig. 16.15** Window support grid dimensions for two common window types (Source: MOXTEK)

6. Plot the data to demonstrate the variation of the intensity as a function of position. Figure 16.16 shows the map from a well-oriented detector plotted using a thermal color scheme in which red represents the highest intensity and blue represents zero intensity. Figure 16.17 shows traverses extracted from the Fig. 16.16 data on diagonals representing parallel to the detector axis and perpendicular to the detector axis. Verify that the most intense region in the intensity plots is in the center of the image area.
7. Note the extent of the region of uniform efficiency. Variation from ideal uniform sensitivity has consequences.
   1. Low magnification X-ray spectrum images will suffer from reduced intensity towards the edges.
   2. Point mode X-ray spectrum acquisitions collected off the optical axis will also suffer from diminished intensities leading to low analytical totals and sub-optimal quantitative results.
   3. Typically, the Cu L-family peak is more sensitive due to absorption by the vacuum window support grid's Si ribs. Figure 16.15 (source: Moxtek) shows the design of two recent Moxtek support grids. The vertical sensitivity is usually minimized by orienting the grid ribs vertically.

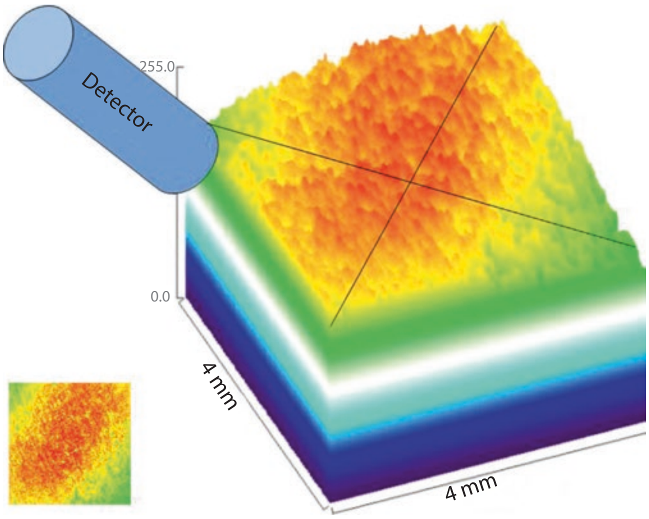

Fig. 16.16 A 3D rendering of the intensity in the Cu K line over a 4 mm by 4 mm mapped area. Created using ImageJ-Fiji

16

Sidebar: Processing a "RAW" Spectrum Image with ImageJ-Fiji

1. Convert the X-ray spectrum image data into a RAW file. A RAW file is large binary representation of the data in the spectrum image. Each pixel in the spectrum image consists of a spectrum encode in an integer binary format. The pixels are organized in a continuous array row-by-row. The size of the file is typically equal to (channel depth) × (row dimension) × (column dimensions) × (2 or 4 bytes per integer value).
2. Import the RAW data file into ImageJ using the "Import → Raw" tools to create a "stack" as shown in Fig. 16.18.
3. As imported, the orientation of the stack will depend upon how the data in the RAW file is organized. Regardless of the original orientation, you will need to pivot the data a couple times using the "Image → Stack → Reslice" tool. First, to identify the range of channels that represent the Cu L-family and Cu K-$L_{2,3}$ intensities. Second, to align the spectrum data with the Z dimension so that the "Image → Stack → Z-project" tool can be used to create plots representing the intensities in the Cu L-family and Cu K-$L_{2,3}$ channels.
4. The initial view of the imported spectrum will usually show the data as shown in Fig. 16.19. In this view it is possible to identify the range of

Fig. 16.17 A plot of two diagonal traverses extracted from the 3D rendering. The *blue dots* are perpendicular to the detector axis and *red* are parallel. Created using ImageJ-Fiji

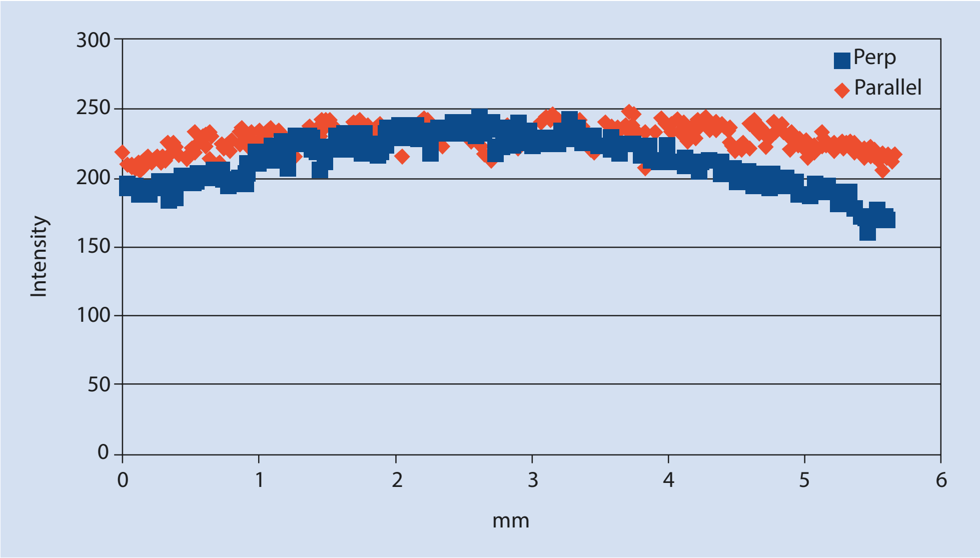

channels to sum together for the Cu L-family and Cu K-$L_{2,3}$ lines. The Cu K-$L_{2,3}$ lines are often quite dim.

5. Using the “Image → Stack → Reslice” tool (see ◘ Fig. 16.20) rotate the stack until it looks like ◘ Fig. 16.21
6. Use the “Image → Stack → Z-project” twice (◘ Fig. 16.22) to extract the range of channels identified in ◘ Fig. 16.19 as associated with the Cu L-family and Cu K-$L_{2,3}$ lines.
7. Convert the gray-scale image to a thermal scale using “Image → Lookup Tables → Thermal.”
8. Convert the image to a plot using “Analyze → Surface Plot”
9. Extract traverses from the image using the straight line tool to define the traverse and then the “Analyze → Plot Profile” tool to extract and plot the data.

16.3.5 Count Rate Linearity

One of the most important circuits in an X-ray pulse processor accounts for the time during which the pulse processor is busy processing X-ray events. When the pulse processor is processing an X-ray, it is unavailable to process new incoming X-rays. This time is called “dead-time.” In contrast, the time during which the processor is not busy and is available is called “live-time.” The sum of “live-time” and “dead-time” is called “real-time” – the time you would measure using a wall clock.

For calculating the effective probe dose, live-time is the critical parameter. The effective probe dose consists of those electrons which could produce measurable X-rays. So the effective probe dose equals the live-time times the probe current. The effective probe dose is always less than the real probe dose, which is the product of the real time and the

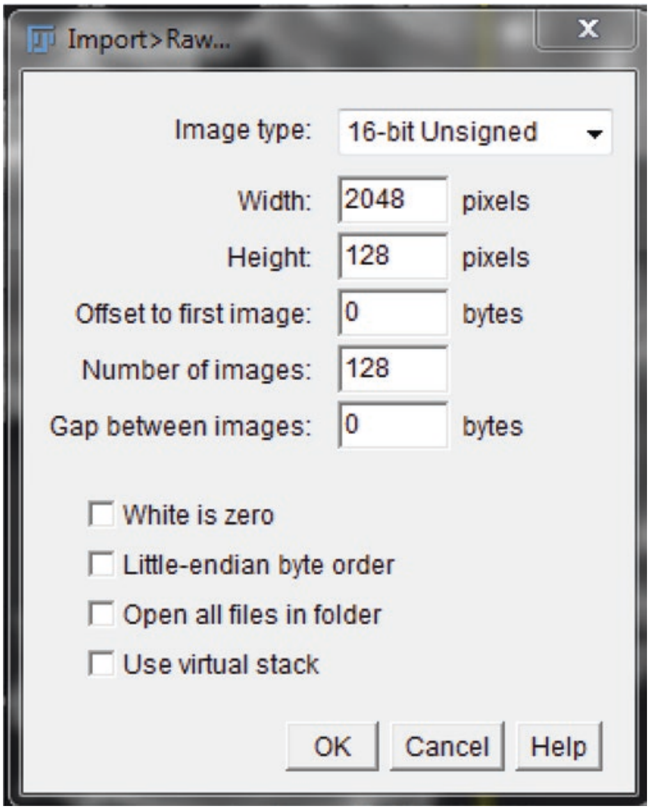

Image type: 16-bit Unsigned
Width: 2048 pixels
Height: 128 pixels
Offset to first image: 0 bytes
Number of images: 128
Gap between images: 0 bytes
☐ White is zero
☐ Little-endian byte order
☐ Open all files in folder
☐ Use virtual stack

◘ **Fig. 16.18** Importing a RAW formatted spectrum image into ImageJ-Fiji

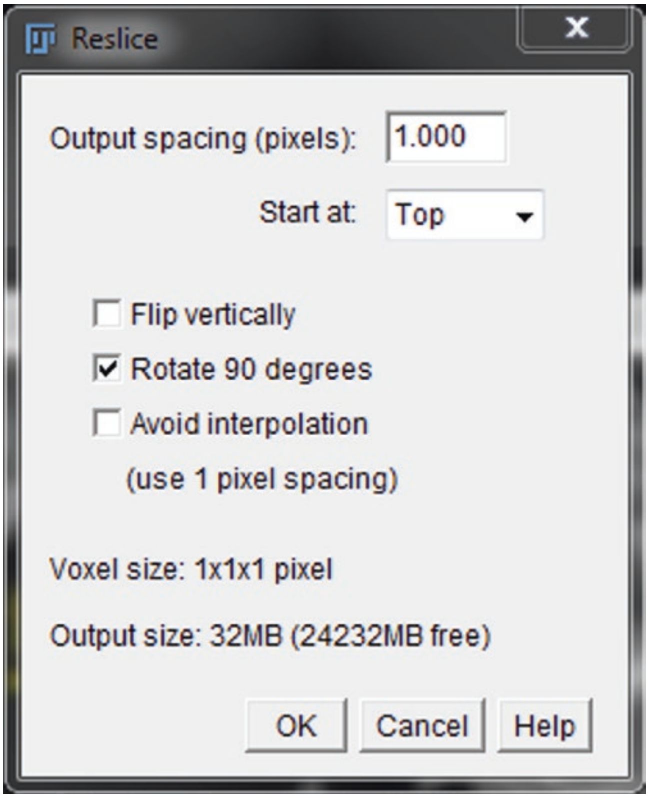

Output spacing (pixels): 1.000
Start at: Top
☐ Flip vertically
☑ Rotate 90 degrees
☐ Avoid interpolation
(use 1 pixel spacing)
Voxel size: 1x1x1 pixel
Output size: 32MB (24232MB free)

◘ **Fig. 16.20** “Reslice” tool used to rotate the stack

◘ **Fig. 16.19** The spectrum image perspective as imported into ImageJ-Fiji. The bright strip is the Cu L-family while the much fainter band is Cu K-$L_{2,3}$

1/1024; 128x128 pixels;

Fig. 16.21 The spectrum image was collected on a 128 by 128 pixel grid representing 4 × 4 mm. After data rotation to view the x-y plane, the first energy slice, 1 out of 1024, is shown. It appears black because it contains no counts

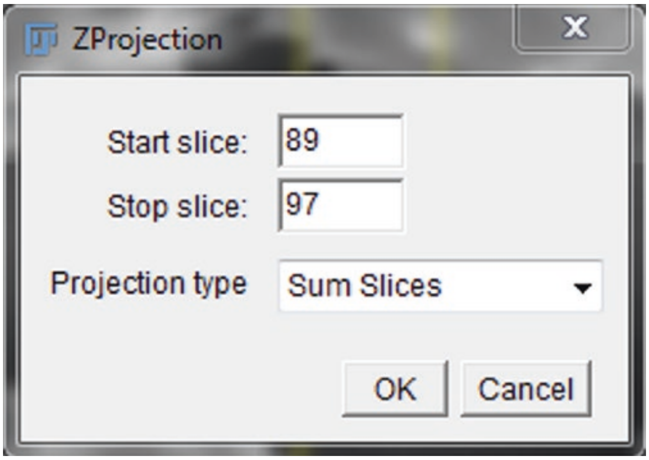

Start slice: 89

Stop slice: 97

Projection type: Sum Slices

Fig. 16.22 Extracting the Cu L-family lines from the spectrum planes 89 to 97

probe current, due to the loss of useful electrons during the dead-time.

It is very important for accurate quantitative analysis that the measured X-ray intensity is linear with respect to the effective probe dose. Twice the effective probe dose should produce twice the measured intensity. Not only is this important because it is often hard to replicate the identical probe current but it is also important because different materials measured with the same probe current will produce different dead times.

There really is no excuse for a modern X-ray detector not to be linear. However, it is worth checking because the test can expose other potential problems like a non-linear or offset probe current meter.

Check 5: Count Rate Linearity with Effective Probe Current

Equipment:

- Faraday cup
- Picoammeter
- Flat, polished copper sample

Procedure:

1. Mount the Faraday cup and the polished copper sample on the stage at the same nominal working distance.
2. Image the sample at the optimal working distance and a beam energy selected in the 15–25 keV range.
3. Start a factor of 10 or more below the optimal probe current. Measure and record the probe current using the Faraday cup and the picoammeter.
4. Collect a 60 live-time second spectrum from the copper sample.
5. Increase the probe current through a sequence of approximately 10–20 steps from the initial probe current to approximately 2 times the optimal probe current. Collect a 60 live-time second spectrum at each probe current and measure and record the probe current using the Faraday cup. A plot of such a measurement sequence is shown in Fig. 16.23 (upper).
6. Integrate the total number of counts in the range of channels representing the Cu K-L$_{2,3}$ characteristic peak. (You don't need to background correct the integral.) Plot the measured intensity divided by the probe current against the measured probe current. The result should be a horizontal line, as shown in Fig. 16.23 (lower).
    1. If the line is not horizontal, the problem may be in the detector or in the probe current measurement.
    2. The probe current measurement could be non-linear meaning the plot of the measured probe current to true probe current is not a straight line.
    3. Alternatively, the probe current may have a zero offset. The zero offset can be measured by blanking the beam and recording the measured current at zero true current. Subsequent probe current measurement can be offset by this value.

16.3.6 Energy Calibration Linearity

Consistent energy calibration is critically important for reproducible quantitative analysis. Pick a nominal channel width (5-eV/channel will work fine in almost all cases) and

Fig. 16.23 The number of X-rays recorded in the spectrum should scale linearly with the dose (the product of live-time and probe current)

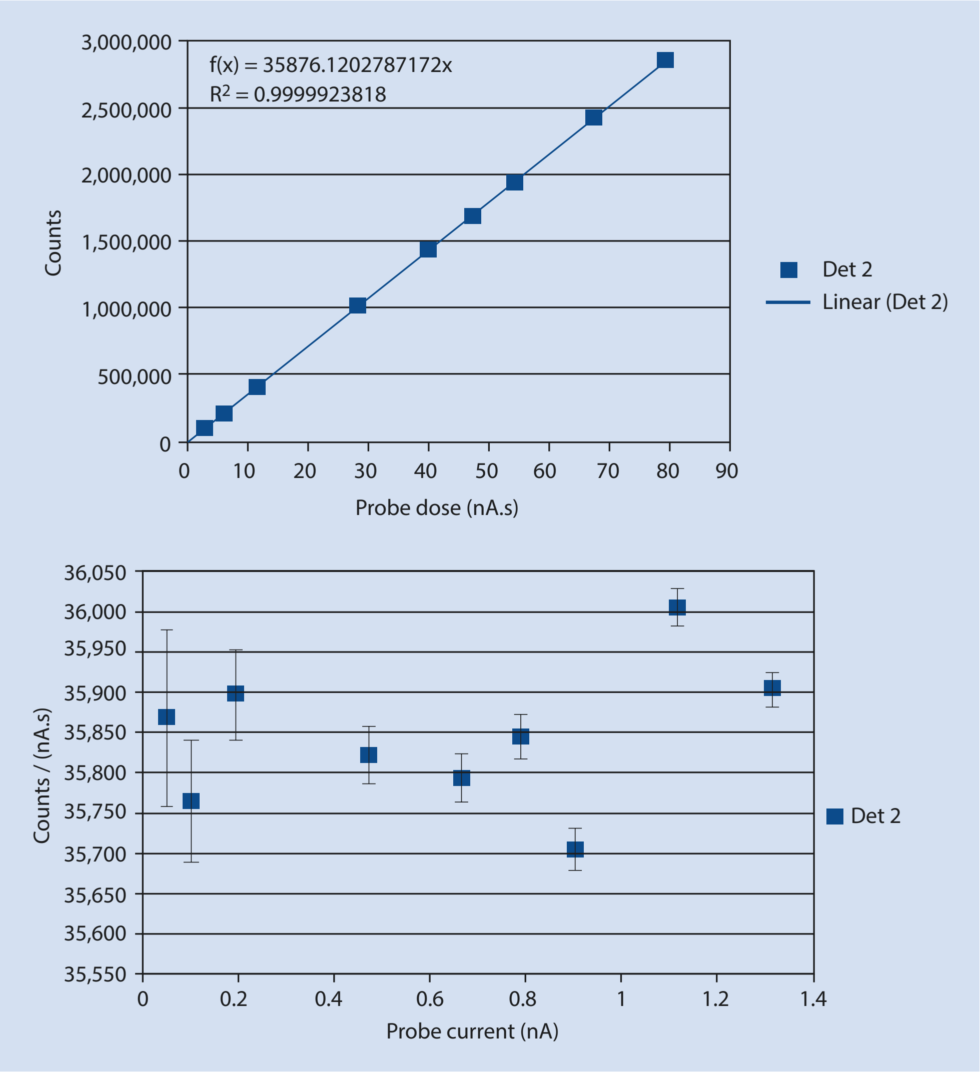

use this value for all your data acquisition. Before each day's measurements ensure that the detector is calibrated consistently by following the same protocol to check and, if necessary, recalibrate your detector.

On a modern pulse processor, calibration is usually performed using the EDS vendor's software. The software will prompt you to collect a spectrum from an established material. The software will examine the spectrum and extract the positions of various characteristic X-ray features. The software will then perform an internal adjustment to center these features in the correct channels. Most modern pulse processors perform a continuous zero offset calibration using a "zero strobe pulse" the pulse processor adds to the signal stream for diagnostic purposes. Thus the only parameter they usually adjust when performing a calibration is an electronic gain. Usually, this involves identifying a single high energy characteristic line (like the Mn K-$L_{2,3}$ or the Cu K-$L_{2,3}$) and adjusting the gain until this feature is centered on the appropriate channel. The calibration is thus a two-point calibration—either a low energy characteristic line or the zero strobe at low energy and a second characteristic line at high energy. Two points are sufficient to unambiguously calibrate a linear function. The calibration (peak position) and resolution (peak shape) should be constant with input count rate (or dead-time), as shown in ◘ Fig. 16.24.

To a very high degree, modern EDS detectors are linear. However if you look carefully in the mid-range of energies, you many notice the KLM markers may be misaligned by a channel or two. This is evidence that your detector is not perfectly linear but this need not represent a true performance problem.

Since energy calibration is so critical but is also one of many parameters that should be measured as part of a complete EDS Quality Control (QC) program, the validation will be discussed in a later section.

16.3.7 Other Items

■ Light Transparency and IR Cameras

Most (but not all) modern EDS detectors have a vacuum tight window that is opaque to infrared and visible light.

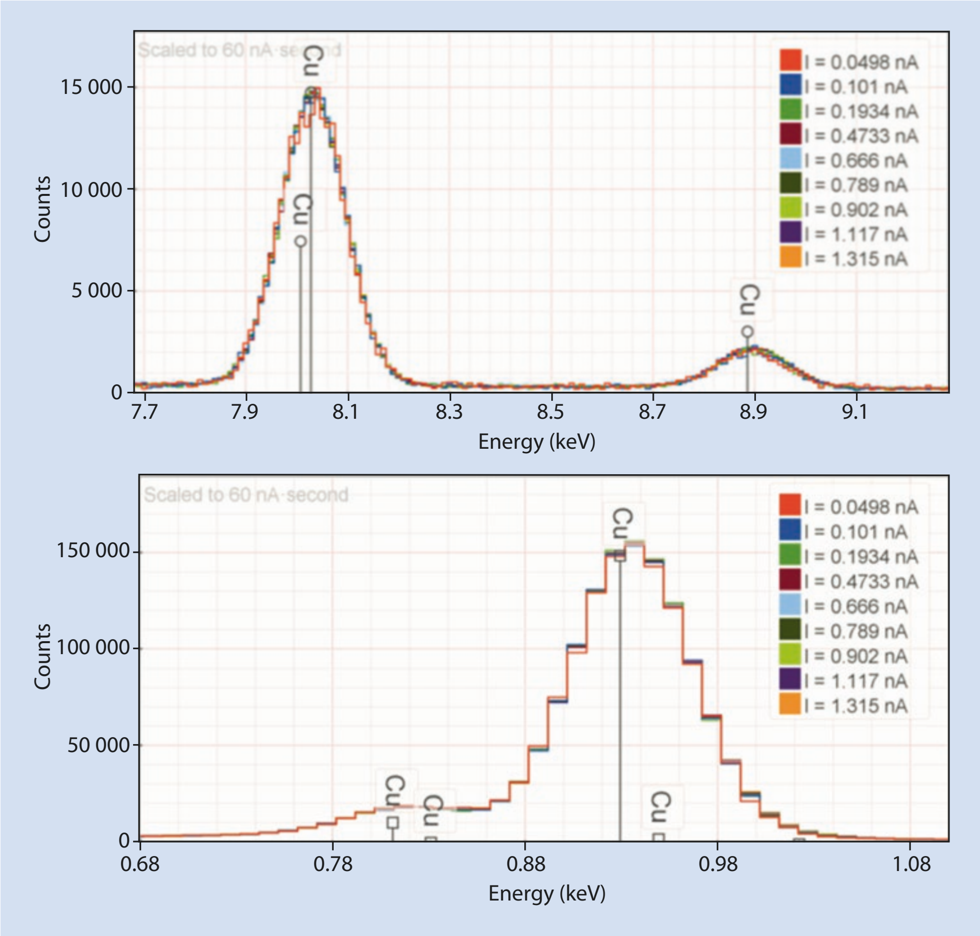

Fig. 16.24 The position and widths of the characteristic peaks should not vary with probe current

Usually, the window is coated with a thin layer of aluminum (or other metal) to keep light in the chamber from creating a spurious signal on the EDS detector.

Regardless, it is worthwhile to test whether your detector is sensitive to light. You may be surprised by a pinhole light leak or a window without an adequate opaque layer.

Check 6: Check for SEM Light Sources

The windows on some EDS detectors are not opaque to light and light in the chamber will produce noise counts particularly in low channels.

1. Enumerate the potential sources of light inside your SEM. Sources to consider:
   1. An IR camera
   2. Stage position sensors
   3. The tungsten filament (essentially a light bulb)
   4. Chamber windows
   5. Cathodoluminescence from samples like zinc selenide or benitoite.
2. Collect a series of spectra and examine these spectra for anomalies.
   1. When possible collect the spectra without an electron beam so there should be no source of X-rays.
   2. Collect a spectrum with the light source turned off and a spectrum with the source on. There should be no difference.

16.3.8 Setting Up a Quality Control Program

An ongoing QC program is a valuable way to demonstrate that your data and results can be trusted——yesterday, today, and tomorrow. If a client ever questions some data, it is useful to be able to go back to the day that data was collected and show that your instrument and detector were performing adequately. A well-designed QC program need not take much time. A single spectrum from a consistent sample collected under consistent conditions is sufficient to identify most common failure modes and to document the long-term performance of your detector. A well-designed QC program is likely to save time by eliminating the possibility of collecting data when the detector is miscalibrated or otherwise misbehaving.

Check 7: Implement a Quick QC Program

1. Maintain a sample consisting of a Faraday cup and a piece of Cu or Mn. Make use of this sample each day on which you intend on collecting quantitative EDS data to ensure that the detector is calibrated.
2. Image the sample at a consistent working distance (the "optimal working distance"), a consistent beam energy, and a consistent probe current.
3. Collect a spectrum from a sample for a consistent live-time.

4. Process the spectrum to extract the raw intensities in the K-$L_{2,3}$ and L-family lines, the resolution, the actual zero offset and gain, and the total number of counts. Record and plot these values on a control chart.

Using the QC Tools Within DTSA-II

While it is possible to implement a QC program by combining an EDS vendor's software with careful record-keeping, DTSA-II provides tools specifically designed to implement a basic EDS detector QC program. The tools import spectra, make some basic sanity checks, process the spectrum to extract QC metrics, archive the metrics and report the metrics.

Creating a QC Project

- A QC project is an archive of spectra collected from a specified sample under similar conditions on a specified detector/instrument. The spectra are fitted with a modeled spectrum and the resulting quantities recorded to track these values over the lifetime of the detector.
- Creating a QC Project involves specifying a detector and the conditions which are to be held consistent (■ Fig. 16.25). If you use a single detector with different process times, either select a constant process time or, better yet, create individual projects for each process time.
  - The material may be simple or complex but should be robust, durable and provide characteristic lines over a large range of energies. Copper is ideal because it is readily available, stable and has both K-$L_{2,3}$ (~8.04 keV) and L-family (~930 eV) lines.
  - The beam energy should be sufficient to adequately excite (overvoltage > 2) all the lines of interest in the sample.
  - The nominal working distance should be the detector's optimal working distance. The sample should be brought into focus (using the stage Z-axis if necessary) at this working distance before collecting a spectrum.
  - The nominal probe current is the probe current at which the spectra will be collected (to within a few percent). Usually, the "use probe current normalization" will be selected so that all intensities are scaled relative to the probe current measured with a in-lens cup or a Faraday cup.
- After creating the project, you will need to go through the QC tool additional times to add measured spectra.

Adding Spectra to a QC Project

- To add spectra to a QC project, you first need to specify which project you will be adding the spectra. Once you select the project, the "material," "beam energy," "nominal working distance," and "nominal probe current" boxes will fill with the associated information (see ■ Fig. 16.26).

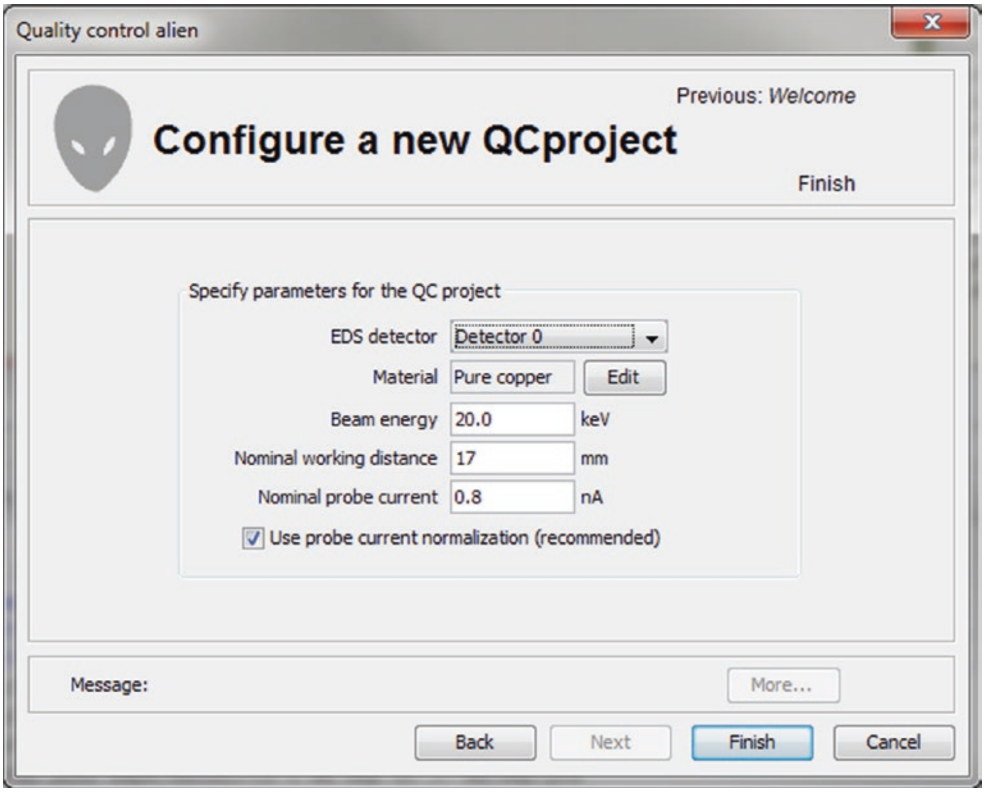

Configure a new QCproject

Specify parameters for the QC project

EDS detector: Detector 0
Material: Pure copper
Beam energy: 20.0 keV
Nominal working distance: 17 mm
Nominal probe current: 0.8 nA
☑ Use probe current normalization (recommended)

Message:

■ **Fig. 16.25** The panel in DTSA-II for creating QC projects. This panel is accessed through the "Tools → QC Alien" menu item

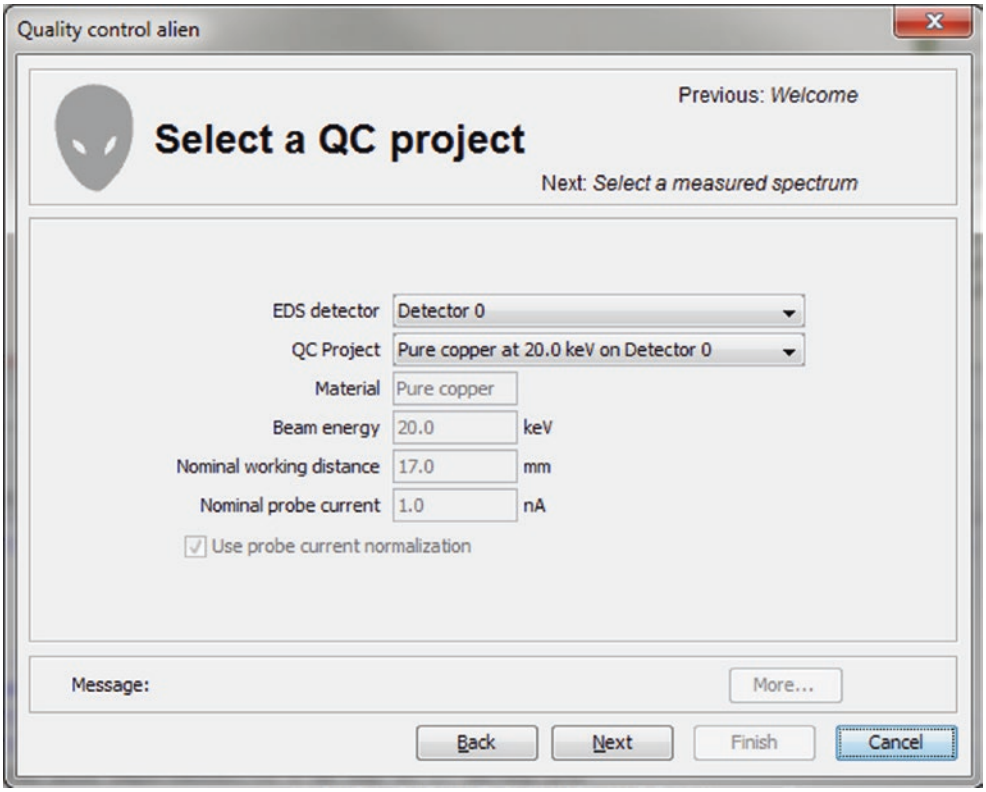

Select a QC project

EDS detector: Detector 0
QC Project: Pure copper at 20.0 keV on Detector 0
Material: Pure copper
Beam energy: 20.0 keV
Nominal working distance: 17.0 mm
Nominal probe current: 1.0 nA
☑ Use probe current normalization

Message:

Fig. 16.26 Panel for selection of detector and material parameters

- Once the project has been selected, you will need to specify a spectrum to add to the project. Needless to say, the spectrum should have been collected on the correct detector under the conditions specified (see Fig. 16.27).
- After selecting the spectrum, the spectrum will be processed by fitting it to a modeled spectrum shape. The resulting fit parameters will be reported and compared with the fit parameters from previous fits. The results are organized into columns associated with the current fit, the average of all fits, average of the first (up to) 10 fits and the average of the last (up to) 10 fits. Review these values to determine whether there has been short or long term drift in any of the fit parameters. The same information is shown in the DTSA-II Report table, as shown in Fig. 16.28.
- You can also generate reports containing these quantities as tabular values, as shown in Fig. 16.29, and plotted on control charts, as shown in Fig. 16.30.

Generating QC Reports

A QC Report is a quick way to track the long-term performance of your detector. QC Reports are also generated using the QC tool accessible through the “Tools → QC Alien” menu item.

You will specify the detector and QC project along with the fit values that you wish to report. The report will be generated into a new HTML document and the result displayed in your system’s default web browser. The report will look like Fig. 16.30, with header information and a series of control charts. At the bottom of the report is a table containing all the data values that went into creating the control charts. All the values computed when the spectrum was added to the QC project will be available to display in the QC report.

16.3.9 Purchasing an SDD

If you were to survey EDS vendor’s advertisements, you’d come to conclusion that two hardware characteristics determine the “best” EDS detector—resolution and detector area. Over the last decade, detector areas have become larger and larger and detector resolutions have improved significantly too. The performance of Si(Li) detectors scaled poorly with size because the detector capacitance scaled with size. SDD, on the other hand, perform only slightly worse (throughput and resolution) as the detector area increases. As a result, even a basic modern SDD-EDS detector is larger and performs better than the best Si(Li)-EDS detector of a decade ago.

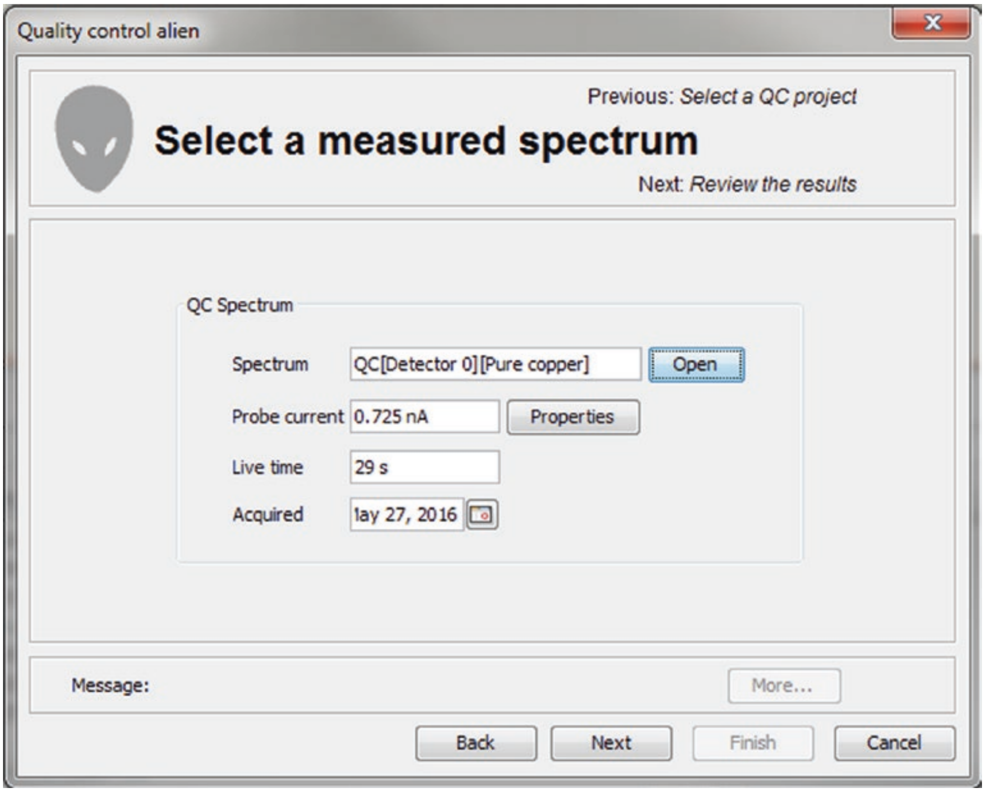

Fig. 16.27 Panel for selection of measured spectrum for archive

Quality control alien

Previous: *Select a QC project*

Select a measured spectrum

Next: *Review the results*

QC Spectrum

Spectrum: QC[Detector 0][Pure copper]

Probe current: 0.725 nA

Live time: 29 s

Acquired: !ay 27, 2016

Message:

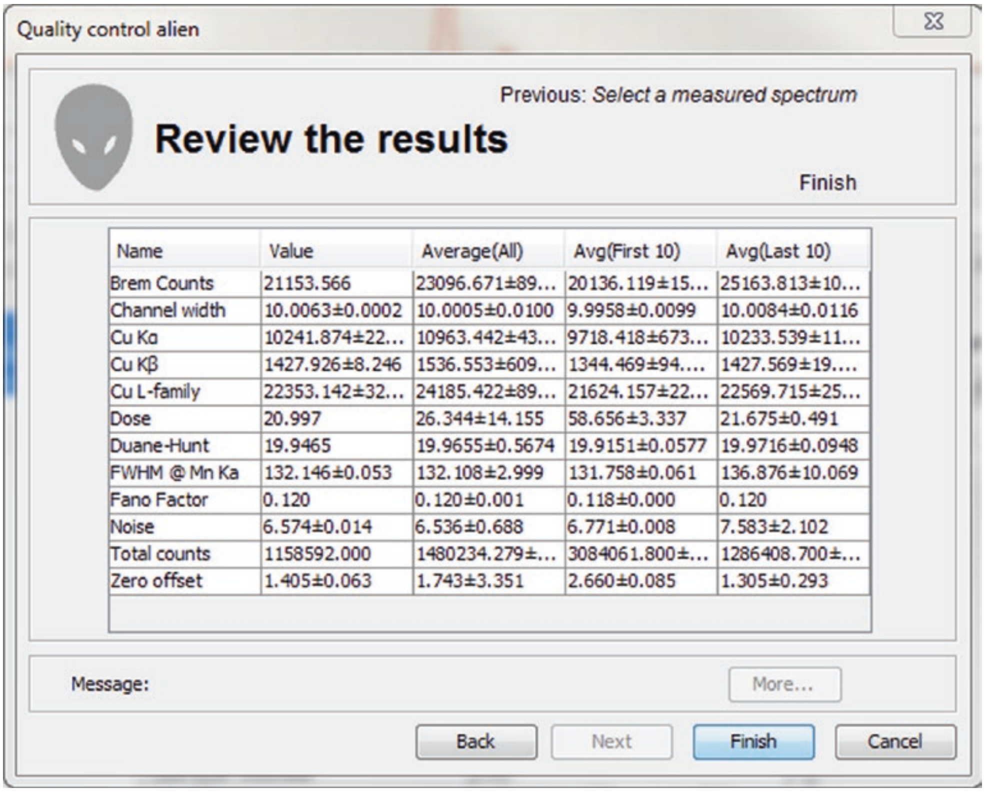

Fig. 16.28 Results of information extracted from measured reference spectrum

Quality control alien

Previous: *Select a measured spectrum*

Review the results

Finish

Name	Value	Average(All)	Avg(First 10)	Avg(Last 10)
Brem Counts	21153.566	23096.671±89...	20136.119±15...	25163.813±10...
Channel width	10.0063±0.0002	10.0005±0.0100	9.9958±0.0099	10.0084±0.0116
Cu Kα	10241.874±22...	10963.442±43...	9718.418±673...	10233.539±11...
Cu Kβ	1427.926±8.246	1536.553±609...	1344.469±94....	1427.569±19....
Cu L-family	22353.142±32...	24185.422±89...	21624.157±22...	22569.715±25...
Dose	20.997	26.344±14.155	58.656±3.337	21.675±0.491
Duane-Hunt	19.9465	19.9655±0.5674	19.9151±0.0577	19.9716±0.0948
FWHM @ Mn Ka	132.146±0.053	132.108±2.999	131.758±0.061	136.876±10.069
Fano Factor	0.120	0.120±0.001	0.118±0.000	0.120
Noise	6.574±0.014	6.536±0.688	6.771±0.008	7.583±2.102
Total counts	1158592.000	1480234.279±...	3084061.800±...	1286408.700±...
Zero offset	1.405±0.063	1.743±3.351	2.660±0.085	1.305±0.293

Message:

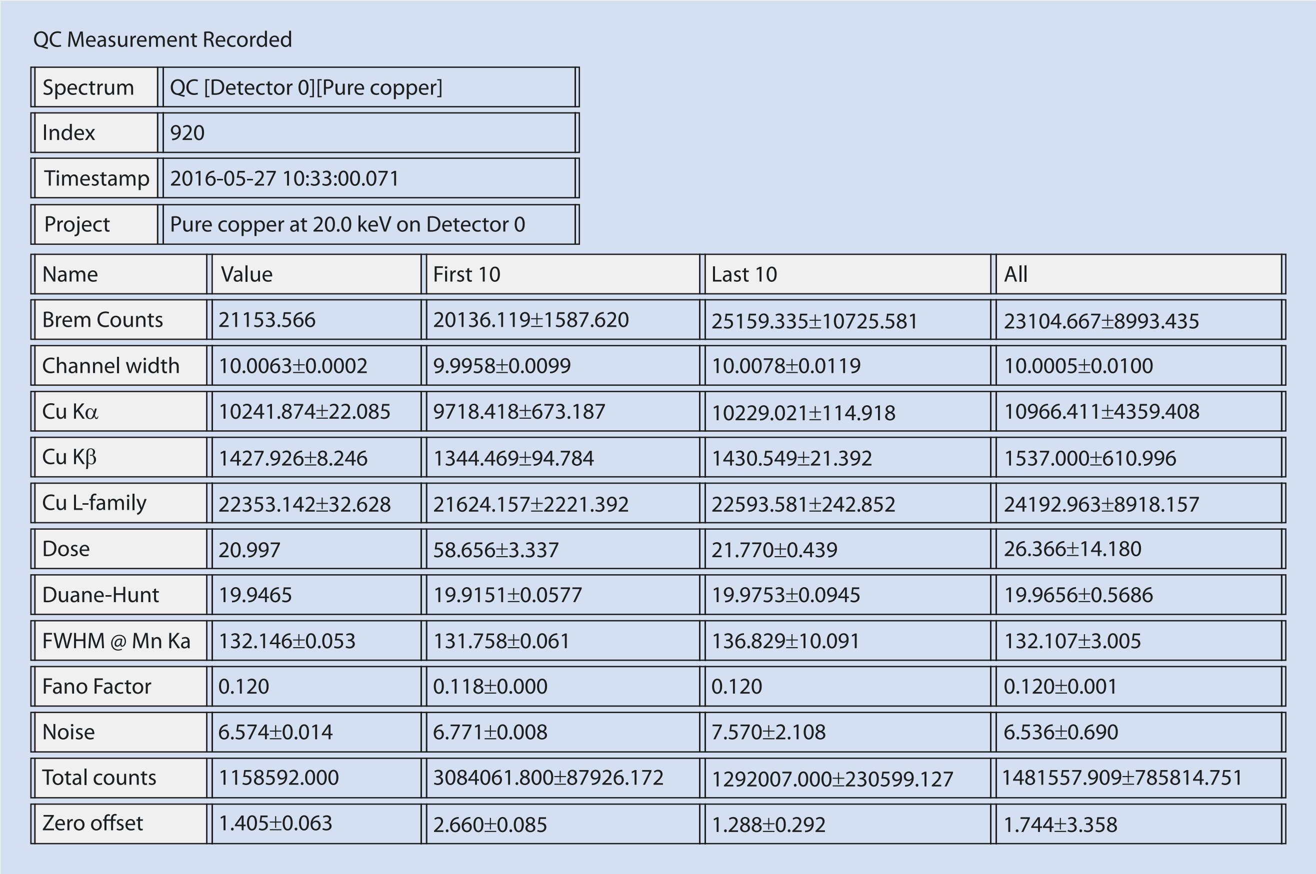

QC Measurement Recorded

Spectrum	QC [Detector 0][Pure copper]
Index	920
Timestamp	2016-05-27 10:33:00.071
Project	Pure copper at 20.0 keV on Detector 0

Name	Value	First 10	Last 10	All
Brem Counts	21153.566	20136.119±1587.620	25159.335±10725.581	23104.667±8993.435
Channel width	10.0063±0.0002	9.9958±0.0099	10.0078±0.0119	10.0005±0.0100
Cu Kα	10241.874±22.085	9718.418±673.187	10229.021±114.918	10966.411±4359.408
Cu Kβ	1427.926±8.246	1344.469±94.784	1430.549±21.392	1537.000±610.996
Cu L-family	22353.142±32.628	21624.157±2221.392	22593.581±242.852	24192.963±8918.157
Dose	20.997	58.656±3.337	21.770±0.439	26.366±14.180
Duane-Hunt	19.9465	19.9151±0.0577	19.9753±0.0945	19.9656±0.5686
FWHM @ Mn Ka	132.146±0.053	131.758±0.061	136.829±10.091	132.107±3.005
Fano Factor	0.120	0.118±0.000	0.120	0.120±0.001
Noise	6.574±0.014	6.771±0.008	7.570±2.108	6.536±0.690
Total counts	1158592.000	3084061.800±87926.172	1292007.000±230599.127	1481557.909±785814.751
Zero offset	1.405±0.063	2.660±0.085	1.288±0.292	1.744±3.358

Fig. 16.29 Report of current QC spectrum measurement parameters compared to archival values

Regardless of what the EDS vendors literature tells us, while both of these performance characteristics are important, neither is the basis of a well-considered choice of detector. Resolution and area are indirect proxies for the performance characteristics that should really drive the decision process—good throughput at an adequate resolution and a large solid angle of detection.

First, a word or two about two characteristics which are absolutely required for good quantitative analysis. Fortunately, almost all modern SDD meet these two important requirements—linearity and stability.

Linearity of Output Count Rate with Live-Time Dose

The number of X-rays measured must be proportional to the number of X-rays generated. If you generated ten times as many X-rays, you should measure ten times as many X-rays. Otherwise, the k-ratio, the basis of all quantitative analysis, would depend not only upon the composition of the material but also the probe current.

Perform the check in section Count Rate Linearity to evaluate a candidate detector's linearity performance.

Resolution and Peak Position Stability with Count Rate

The detector resolution and peak position must not change appreciably with a variation of a factor of ten or more in X-ray flux.

The same spectra used to demonstrate linearity can be used to demonstrate peak position and resolution stability. Use DTSA-II's calibration tool to fit the spectra and extract full width at half-maximum (FWHM) and channel width values for each spectrum. Plot the spectra and results as shown in Fig. 16.31.

Having ensured these two basic characteristics, the choice of next most important characteristic depends upon how your detector will be used. If signal quantity is a problem because you are limited to low probe currents, STEM mode analysis of microparticles, low beam energy analysis, or another reason why the flux of X-rays is limited, then a detector that maximizes solid angle is important. If on the other hand, you can produce a lot of X-rays, then throughput at an adequate resolution is more important. Regardless, both criteria should be part of your evaluation process.

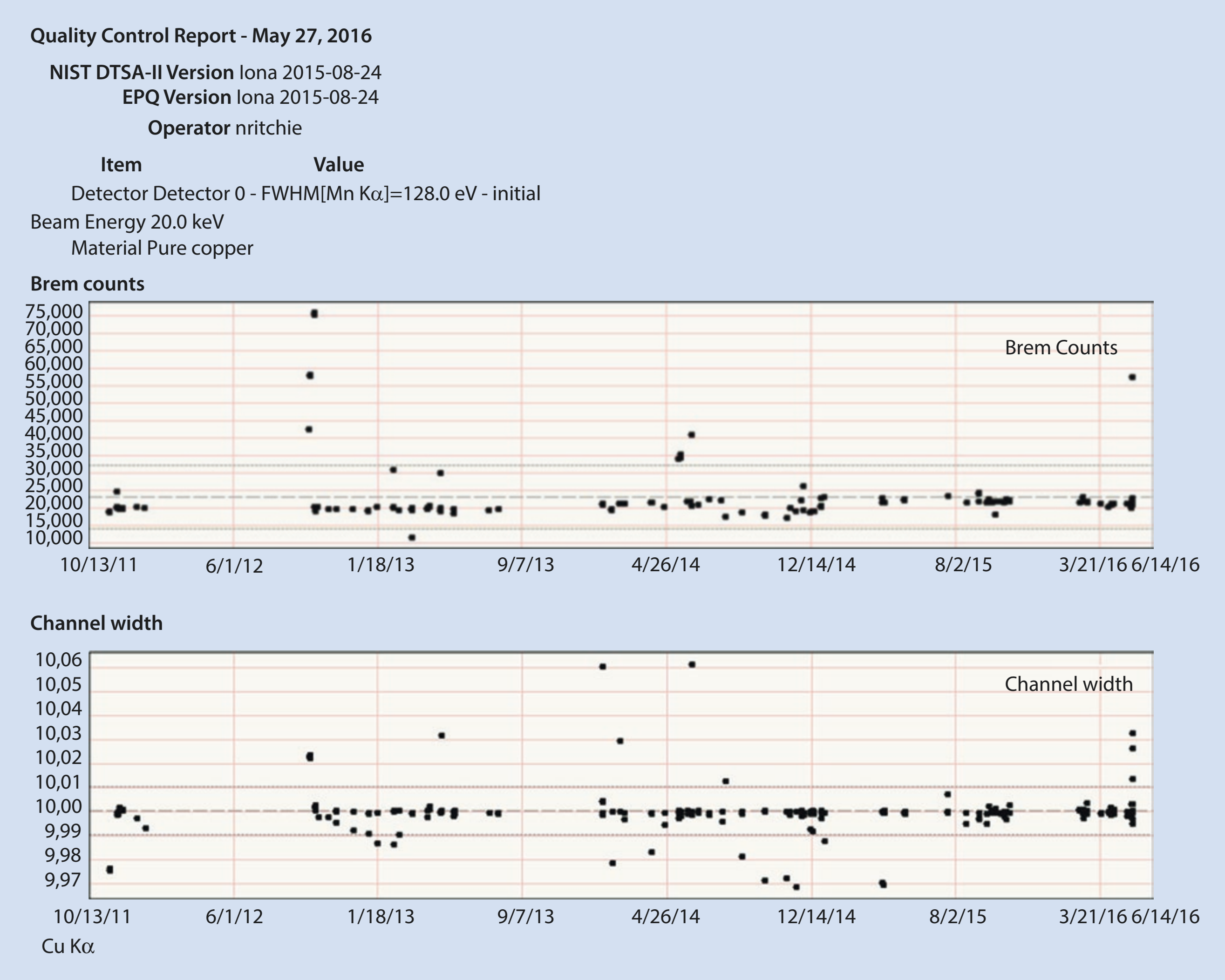

Quality Control Report - May 27, 2016

NIST DTSA-II Version Iona 2015-08-24
EPQ Version Iona 2015-08-24

Operator nritchie

Item	**Value**
Detector	Detector 0 - FWHM[Mn Kα]=128.0 eV - initial
Beam Energy	20.0 keV
Material	Pure copper

Brem counts

Channel width

Cu Kα

Fig. 16.30 Quality control report charts

Fig. 16.31 Neither the resolution (FWHM at Mn K-$L_{2,3}$ (Kα)) or the gain (in eV/channel) should change with probe current

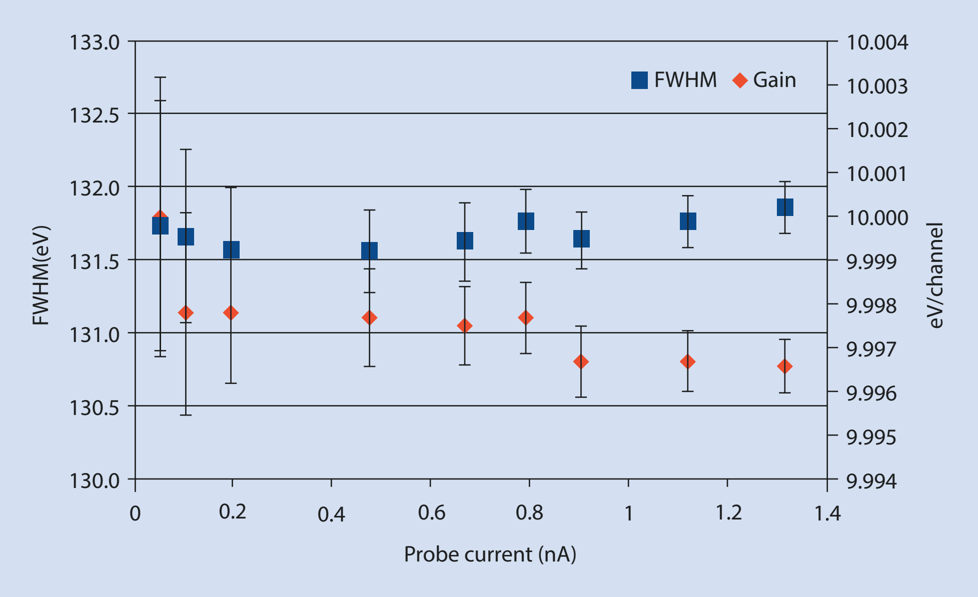

Solid Angle for Low X-ray Flux

The fraction of X-rays emitted by the sample that strike the detector is proportional to the solid angle. The solid angle is a function of both the active area of the detector and the distance from the sample to the detector. The detected fraction is linearly proportional to the active area of the detector but inversely proportional to the square of the distance from the sample to the detector so the position of the detector is critical. It is not reasonable to assume that a larger area detector will always produce a larger solid angle. Larger area detectors may require larger diameter snouts which may not be able to be positioned as close to the sample. Larger area detectors may also produce slightly poorer resolution and/or slightly lower ultimate throughput due to increases in “ballistic deficit” — the spreading of electron packets in the active detector area.

The only way to know ahead of time what solid angle you can expect is to ask they vendor to provide schematics showing how your detector will be positioned in your instrument. The critical parameters are sample-to-detector distance at the maximum insertion position, the optimal working distance, the detector area, and the elevation angle. These parameters can be used within DTSA-II to model the X-ray signal you can expect to measure from the types of samples and the probe currents you use.

Maximizing Throughput at Moderate Resolution

Modern detectors are capable of extraordinary resolutions and high throughput, though not both at the same time. The best resolutions are achieved at long pulse process times, which produce poor ultimate throughput. The highest throughputs are achieved at short pulse process times; but, while it may be possible to measure many X-rays per unit time, coincidence events (pulse pile up) limit the quantitative accuracy. The quantitative performance of the detector is three-way trade-off between throughput, resolution, and coincidence rate. Typically, this is accomplished by defining an acceptable coincidence rate as discussed in the section on process time and determining the process time that maximizes the throughput at this coincidence rate. This process time will typically be a slight compromise from the one that produces the optimal resolution but typically not by more than a few eV FWHM at Mn K-$L_{2,3}$ (Kα). A few eV of resolution degradation is usually an acceptable compromise as throughput is far more important than resolution for accurate quantitative EDS microanalysis.

Special Case: Low Energy Sensitivity

If measuring low energy X-rays in the sub-200-eV range is particularly important to you, then you should focus your criteria on this energy region and understand that to optimize this regime will likely require compromises to throughput. Find samples similar to the ones you will commonly measure and use these samples to evaluate the performance of the candidate detectors.

References

Fiori C, Newbury D (1978) Artifacts in energy dispersive X-ray spectrometry. Scan Electron Microsc 1:401

Fitzgerald R, Keil K, Heinrich KFJ (1968) Solid-state energy-dispersive spectrometer for electron-microprobe X-ray analysis. Science 159:528

Gatti E, Rehak P (1984) Semiconductor drift chamber – an application of a novel charge transport scheme. Nucl Instr Meth A 225:608

Struder L, Fiorini C, Gatti E, Hartmann R, Holl P, Krause N, Lechner P, Longini A, Lutz G, Kemmer J, Meidinger N, Popp M, Soltau H, Van Zanthier C (1998) High-resolution high-count-rate X-ray spectroscopy with state-of-the-art silicon detectors. Mikrochim Acta Suppl 15:11